NASA TECHNICAL NOTE

NASA TN D-5864
C.1

NASA TN D-5864

VACUUM LEAKAGE TESTS OF A SIMULATED LIGHTWEIGHT SPACECRAFT AIR LOCK

by Otto F. Trout, Jr.

Langley Research Center
Hampton, Va. 23365

NATIONAL AERONAUTICS AND SPACE ADMINISTRATION • WASHINGTON, D. C. • JULY 1970

1. Report No. NASA TN D-5864	2. Government Accession No.	3. Recipient's

4. Title and Subtitle VACUUM LEAKAGE TESTS OF A SIMULATED LIGHTWEIGHT SPACECRAFT AIR LOCK	5. Report Date July 1970
	6. Performing Organization Code

7. Author(s) Otto F. Trout, Jr.	8. Performing Organization Report No. L-7282

9. Performing Organization Name and Address NASA Langley Research Center Hampton, Va. 23365	10. Work Unit No. 124-08-18-01
	11. Contract or Grant No.

12. Sponsoring Agency Name and Address National Aeronautics and Space Administration Washington, D.C. 20546	13. Type of Report and Period Covered Technical Note
	14. Sponsoring Agency Code

15. Supplementary Notes

16. Abstract

A lightweight simulated spacecraft air-lock structure was tested under high vacuum to evaluate structural sealing problems and to determine leakage rates. Three different types of hatch configurations and three different seal configurations were tested for a temperature range of from -40° F (-40° C) to 200° F (93° C). Leakage rates of less than 1×10^{-4} cc/sec or less than 10 cc/day of helium (standard temperature and pressure) were attained for each hatch.

17. Key Words (Suggested by Author(s)) Air lock Seals Spacecraft structure	18. Distribution Statement Unclassified — Unlimited

19. Security Classif. (of this report) Unclassified	20. Security Classif. (of this page) Unclassified	21. No. of Pages 45	22. Price* $3.00

*For sale by the Clearinghouse for Federal Scientific and Technical Information
Springfield, Virginia 22151

VACUUM LEAKAGE TESTS OF A SIMULATED
LIGHTWEIGHT SPACECRAFT AIR LOCK

By Otto F. Trout, Jr.
Langley Research Center

SUMMARY

A lightweight simulated spacecraft air-lock structure was tested under high vacuum to evaluate structural sealing problems and to determine leakage rates. Three different types of hatch configurations and three different seal configurations were tested for a temperature range of from -40° F (-40° C) to 200° F (93° C). Leakage rates of less than 1×10^{-4} cc/sec or less than 10 cc/day of helium (standard temperature and pressure) were attained for each hatch except in one case where the hatch seal appeared to unseat as a result of structural deformations caused by temperature differentials in combination with the unsymmetrical hatch.

INTRODUCTION

The National Aeronautics and Space Administration is conducting advanced research on air-lock systems and associated structural seals applicable to future space vehicles. Extended manned orbital and interplanetary space flights require highly reliable lightweight sealing concepts for efficient long-term containment of a habitable atmosphere. Reliable air-lock systems through which the astronauts can egress to perform extravehicular operations are also necessary. Studies were started several years ago to develop the technology for sealing large-diameter lightweight spacecraft structures, the results of which are reported in references 1 to 4. Additional studies were undertaken to define air-lock geometry, pumping systems, and human factors constraints, the results of which are reported in references 5 to 9.

Reference 4 indicates that acceptable leakage rates for atmospheric confinement are possible, but not proven, for large lightweight structures with commercially available elastomeric seals provided the following conditions are met: (a) the seal materials and flanges are free of defects, (b) a seating stress above the minimum acceptable value for vacuum use is maintained along the entire length of the seal during all dynamic and static structural loading and deformation conditions, (c) the seals are protected against ultraviolet, electromagnetic, and particulate radiation, and (d) the seals are protected against both high and low temperatures.

To verify further the structural seal concepts and to apply them to large structures for which research data were not available, an investigation was conducted on the use of large-diameter O-rings of butyl, neoprene, viton, and silicone elastomers. The results of this study are reported in reference 10. Leakage rates were in agreement with data from small-diameter seals and approached that of the permeability of the basic elastomeric polymer as reported in reference 4.

Further development of the technology required that research be conducted on lightweight structures. Therefore, a program was undertaken to design, construct, and test a full-size lightweight air-lock system to study leakage and associated operational problems. The air lock resulting from this effort is shown in the photograph in figure 1. A modification of this air lock was proposed for the Air-Lock experiment for Saturn S-IVB/SA-209 (later called S-IVB Workshop). (See ref. 11.)

The air lock was constructed to facilitate the study of a wide variety of problems associated with an air lock mounted either on the exterior or interior of the spacecraft, or as a connecting air lock between two space vehicles. Three different geometric hatch configurations were studied on the air lock and each configuration had a characteristic seal, either an O-ring, a molded seal, or an inflatable seal. The details of each hatch configuration and seal type are discussed.

Leakage tests were performed on each of the air-lock hatches with atmospheric pressure on one side and a vacuum of approximately 10^{-6} torr on the other side. Leakage measurements were made by methods described in reference 10. Additional leakage measurements were made with the hatches at temperatures from -40° F (-40° C) to 200° F (93° C). Leakage measurements are reported at standard conditions of temperature and pressure.

The present paper describes structural details of the lightweight air lock, the leakage tests conducted thereon, and a compilation of the test results.

APPARATUS

Simulated Spacecraft Air Lock

Figure 1 shows the air lock mounted on the storage and shipping stand. This model consisted of two main cylindrical sections each having an internal diameter of 48 inches (1.22 meters) and a combined length of 81 inches (2.06 meters) when joined together. The air lock has a total mass of 377 pounds (171 kilograms) excluding the lighting and communication system and the storage and shipping stand.

Three different concepts of ingress-egress hatches were built into the air-lock system. A circular configuration (hatch A, fig. 1) in a concentric hatch frame was

designed to provide for symmetrical loading of both the hatch and hatch frame. Symmetrical loading is desirable from the standpoint of efficient lightweight structural design, ease of predicting structural loads, and minimum deflections.

An oblong configuration (hatch B) at the opposite end of the air lock was designed to provide unsymmetrical loading of the hatch and hatch frame. Since not all structures are amenable to symmetrical design, hatch B was designed to investigate some of the structural sealing problems associated with nonuniformly loaded structures.

A circular hatch having a cylindrical contour (hatch C) was included on the side of the air lock. This hatch was designed and built to investigate the feasibility of and the sealing problems associated with a hatch which seals a contoured surface.

Each of the hatches was provided with both a latching mechanism and a pressure equalization valve, both of which were operable from either the inside or the outside of the air lock. Pressure gages similar to that shown in figure 2 were provided on both sides of each hatch to indicate differential pressure across the hatch during air-lock operation. A lighting and communication system (fig. 1) was installed on the inside of the air lock but was not used in the present tests. The hatch frames at each end of the air lock could be unbolted from the cylindrical shell, turned 180°, and reattached with bolts and clamps so that the hatch could be pressure loaded in the opposite direction.

All air-lock surfaces and mechanical parts which made contact with other surfaces were plated with electrodeposited molybdenum disilicide to prevent cold welding in vacuum conditions and for lubrication.

The air-lock system was designed to be operated at either an external or an internal differential pressure of 1 atmosphere, with a design safety factor of 1.5 on yield (1 atmosphere = 1×10^5 N/m^2). Further details on the structural design stress analysis of the air-lock system and the associated components are available in reference 12. The air-lock system was designed for a minimum service life of 1000 cycles of pressurization and hatch actuation. Further information on operational and maintenance procedures for the air-lock system are presented in reference 13. A summary of the masses of the various components of the air lock is presented in table I.

Cylindrical Shell Details

The outer cylindrical shell of the air lock consisted of two sections, one 60-inch (1.53-meter) length and the other 21-inch (0.53-meter) length. Each section had flanges so that it could be installed on the inside or the outside of the mounting flange of the vacuum test chamber. The two cylindrical shell sections were constructed of 2014-T6 aluminum plates which were milled to a wall thickness of 0.062 inch (1.57 mm) and stiffened with integral stringers, rolled to the cylindrical contour, and welded to form the

cylinder. The frame for hatch C was integral with the cylinder. An additional skin thickness of 0.062 inch (1.57 mm) was provided around the hatch C frame for reinforcement.

Hatch A Details

Figure 2 presents a photograph of hatch A and its retaining frame. Hatch A was 32 inches (0.81 meter) in diameter. Both the hatch and frame were constructed of 2014-T6 aluminum. A core cavity was "milled out" and filled with aluminum honeycomb bonded to the outer sheets as illustrated in figure 3. The wall between the honeycomb core and the hatch exterior surfaces was 0.040 inch (1.01 mm) thick on both the hatch and hatch frame. The honeycomb was sealed between the walls of the structure to prevent outgassing of the epoxy into the air lock.

The latching of hatch A was by a modified breech block mechanism consisting of cam rollers mounted on a rotating rim and actuated by a lever-type handle on each side of the hatch. Some of the pertinent details are shown in figure 3. A safety mechanism was provided so that the hatch could not be opened unless the pressure-equalization valve was open. The latching mechanism could be actuated from either side of the door.

Hatch A was sealed to the hatch frame when in the closed position by a single captured butyl O-ring seal seated in a trapezoidal groove. The details of this seal are shown in figure 3. This configuration was designed to provide a 15-percent linear deformation of the O-ring cross section when the hatch was closed and latched. The hatch-actuation shaft which penetrated the hatch was also sealed with butyl O-rings.

Details of the pressure-equalization valve are shown in the diagram in figure 4. The valve could be actuated from either side of the hatch by turning the actuation handle. An acme screw thread clamped the seal plate against the hatch. Sealing between the valve and the hatch was provided by a molded seal bonded to the seal plate. A deflection plate was provided next to the valve handle to prevent air from directly striking the person opening the valve. The valve was designed to provide equalization of the pressure between the interior and exterior of the air lock in a period of 10 seconds.

Figure 5 presents a diagram of the details of the window in hatch A. The window consisted of two circular layers of tempered glass with a bonded silicone rubber safety interlayer. The window was sealed by a single butyl O-ring.

Hatch B Details

Figure 6 presents a photograph of hatch B. It was an oval configuration 30 inches (0.76 meter) wide by 36 inches (0.92 meter) high. Both the hatch and hatch frame were constructed of 2014-T6 aluminum with a milled out cavity bonded to the aluminum honeycomb core and an aluminum sheet bonded over the honeycomb. The wall thickness between

4

the honeycomb core and the hatch exterior surfaces was 0.040 inch (1.01 mm), except that the exterior surface of one side of the hatch frame was 0.080 inch (2.02 mm) thick.

The latching mechanism for hatch B consisted of two semicircular wedge-type expanding rings in the door actuated by a lever system connected to the latching handle control wheel in the center of the hatch as shown in figures 7 to 9. The rotary handle turns the spiral track plate on the reverse side and actuates the cam roller follower which, in turn, moves the push-pull actuation levers. (See fig. 8.) The push-pull actuation lever actuates the expander linkage which, in turn, causes the expander rings to extend uniformly around the periphery of the hatch. When the push-pull actuation lever is fully extended, the expander linkage is in an over-center position; thus, the two expander rings are locked in an extended position. When the expander rings are fully extended, they force the hatch against the hatch frame and deform the seal on its mating surface, as shown in figure 8. Figure 9 shows a cross section of the expander ring in the retracted position.

The molded-type seal (fig. 9) was a commercial butyl elastomer bonded to both sides of a retainer plate. The retainer plate was fastened to the hatch with screws. When the hatch was fully closed, the elastomeric seal was deformed to a level even with the metal retainer plates.

The details of the pressure equalization valve for hatch B were similar to those of hatch A, shown in figure 4, except that a larger airstream deflection plate was used on the outside of the door, as shown in figure 6.

As a safety feature, the latching handle of hatch B could not be turned to unlatch the hatch unless the pressure-equalization valve was opened. This feature was made possible by an indentation in the spiral track plate into which the pressure-equalization valve deflection plate fits when the valve is closed, as shown in figure 6. Differential-pressure gages were provided on each side of hatch B identical to the ones used on hatch A.

Hatch C Details

Figure 10 presents a photograph of hatch C as mounted on the outside of the cylindrical section of the air lock. It was a circular configuration 36 inches (0.92 meter) in diameter, and had a cylindrical contour to match the outside diameter of the air-lock cylinder. The hatch was constructed of 2014-T6 aluminum milled out to a cross-section thickness of 0.040 inch (1.01 mm) with an aluminum honeycomb core placed in the milled recess and an 0.040-inch (1.01-mm) sheet of 2014-T6 aluminum bonded to the exterior surface as shown in figure 11.

The hatch could be manually moved along a track which conformed to the outside contour of the air-lock cylinder in order to open and close it as illustrated in figure 1. In the closed position a tongue protruded toward the inside of the hatch periphery and

5

engaged the retainer lip on the lower side of the hatch. A similar lip protruded outward from the hatch periphery to engage another lip, as illustrated on the lower and upper cross sections in figure 11. A latching mechanism retained the hatch in place during inflation of the seal. The entire pressure loading on the hatch is carried by this tongue and retained lip arrangement.

The pressure-equalization valve was similar to the ones for hatches A and B, except that the valve incorporated a safety latching mechanism which retained the hatch in place when the valve was closed, as illustrated in figure 11.

The butyl elastomeric inflatable seal was held in place by retainer clamps. The inner part of the seal was inflated with gaseous nitrogen to 30 psia (20.68×10^4 N/m^2) to expand it against the hatch.

Test Chamber Installation

Figures 12 and 13 show a typical installation of the flight-weight air lock in the vacuum seals test chamber at the Langley Research Center. In the installation shown here, the 60-inch (1.53-meter) length cylindrical section was mounted on the exterior of the test chamber whereas the 21-inch (0.53-meter) length section was mounted on the interior. The cylindrical sections were attached to both the interior and exterior of the test chamber by a series of clamps as shown in figure 12 so that the cylindrical shells could be pressure loaded with either external or internal pressure. The air-lock cylindrical sections were each sealed to the mounting plate by a separate O-ring. For some of the tests the larger cylindrical section was mounted on the interior of the test chamber and the shorter section on the exterior. In addition, the frames of hatch A and hatch B were reversible on the cylindrical section; that is, they could be turned 180° and reattached to the cylinder so that the hatches and frames could be pressure loaded in the opposite direction.

A description of the vacuum seals test chamber and the associated performance characteristics is presented in reference 10. The chamber is 8 feet (2.44 meters) in diameter and 8 feet (2.44 meters) long and has a vacuum system capable of pumping the chamber to 1×10^{-7} mm Hg under conditions of no leakage (1 mm Hg = 1.333×10^2 N/m^2).

Figures 12 and 14 show the isolation blankets which were used to flood specific enclosed areas with helium to determine leakage of that area of the air lock at room temperature. This technique is a refinement of the system used in reference 10. Figure 14 shows the isolation blanket used on hatches A and B (hatch B shown). It was attached to the hatch frame with a circumferential clamp. Figure 12 shows the isolation blanket installed on hatch C. An inlet and outlet were provided so that residual air could be evacuated with a vacuum pump and helium injected into the enclosed area.

Figures 15 and 16 show the arrangement used to heat hatches A and B to temperatures above 200° F (93° C) during leakage tests. Twelve critical points on the inside and the outside of the hatch and hatch frame were instrumented to measure temperatures during the tests. The output of the thermocouples was recorded on a strip chart recorder as shown in figure 16.

The heat lamps and hatch were enclosed in a reflective insulating cover, as shown in figure 16. The cover also served as an isolation blanket for injection of helium into the confined area for leakage measurements.

Figure 17 shows the installation of the heat lamps and thermocouples on hatch C before installation of the insulating cover. Figure 18 shows hatch C enclosed for the heating tests. Temperatures on hatch C were controlled in the same manner as on hatches A and B.

Figures 19 and 20 show the arrangement used during the low temperature tests to cool hatch B to -40° F (-40° C). (The same arrangement was used for hatch A.) Liquid nitrogen was evaporated in copper coils attached to a cold plate located approximately 4 inches (0.1 meter) from the surface of the hatch. (See illustration in fig. 19.) The insulating-reflective blanket shown in figure 20 was used to prevent heat from the surrounding air from entering the cooled area. The blanket also served to isolate the enclosed area over the hatch from the injection of helium for the leakage measurements. The same thermocouples as used on the heating tests were used in the cold tests. Temperature of the hatch was controlled by manually controlling the flow of liquid nitrogen into the cooling coils.

Figures 21 and 22 show the arrangement used to cool hatch C. The cooling coils were placed approximately 0.5 inch (1.2 cm) from the hatch surface as illustrated in figure 21, and then enclosed in an insulating blanket as shown in figure 22. Temperature was controlled by adjusting the flow of liquid nitrogen through the cooling coils. Thermocouples connected to a strip chart recorder were used to record temperature as a function of time.

TESTS AND MEASUREMENTS

Prior to acceptance of the air lock from the contractor, the air lock was tested and satisfied the leakage test criteria listed in table II. In addition, a structural integrity test was performed by pressurizing the air lock to 1.2 atmospheres differential internal pressure. Additionally, a test subjecting the exterior to an external differential pressure of 1.2 atmospheres was made with the interior evacuated.

After acceptance of the air lock from the contractor, a series of leakage measurements was made in greater detail with the air lock mounted in the vacuum seals test

chamber. (See fig. 12.) In this case the 60-inch (1.53-meter) cylindrical section was mounted on the exterior of the test section and the 21-inch (0.534-meter) section was mounted on the interior of the test chamber. For tests on hatch C with atmospheric pressure on the interior of the air lock and the exterior evacuated, the 60-inch (1.53-meter) cylindrical section was mounted on the interior of the test chamber and 21-inch (0.534-meter) section on the exterior. During the tests the vacuum test chamber was pumped to a vacuum of approximately 1.0×10^{-6} torr (1 torr = 1.33×10^2 N/m^2).

Leakage was measured by methods presented in reference 10. Briefly, the method consists of enclosing the area to be measured in an isolation blanket as shown in figures 12, 14, 16, and 18 and then flooding the enclosed area with helium. The rate of helium leakage to the inside of the test chamber is determined with a helium mass spectrometer. This system is used to measure leakages as small as 1×10^{-7} cc/sec on large systems. Calibration against known leakage sources are repeatable to within ±5 percent under stable outgassing conditions. A detailed discussion of the accuracy and sources of error using the present system is presented in reference 10. Since permeation of helium through elastomeric seals required a finite time to reach equilibrium, each test was continued for a period of from 2 to 3 hours. Except for the temperature tests reported in table II, all tests were performed at room temperatures between 70° F (21° C) and 80° F (27° C).

Leakage tests were performed at temperatures up to 200° F (93° C) on hatches A, B, and C and down to -40° F (-40° C) on hatches B and C by using the apparatus previously described. The lower temperatures were dictated by the performance of the available equipment.

RESULTS AND DISCUSSION

Table III lists a summary of pertinent leakage tests performed on the air lock by using the helium measuring methods described in reference 10. The leakage of helium would be greater than that for higher molecular gases such as air. For the low leakage rates encountered in these tests, air leakage cannot be measured directly by the present system since a single leak cannot be isolated for purposes of measurement from the other leakage sources and outgassing products.

Room Temperature Tests

Figure 23 presents the leakage rate of the butyl O-ring seal in hatch A with pressure loading the hatch toward the closed position after 1 and after 50 cycles of hatch actuation. The maximum leakage was relatively small, 3.1×10^{-6} cc/sec after 1 cycle and 1.0×10^{-5} cc/sec after 50 cycles. This leakage was less than 1 cc/day for the entire

8

hatch and the hatch frame. In this case, about a 50-percent increase in leakage occurred after 50 cycles.

Figure 24 presents the leakage rate of hatch A with pressure loading toward the open position after 1 cycle and after 50 cycles of hatch actuation. Maximum leakage after 1 cycle was 6.2×10^{-6} cc/sec and after 50 cycles 2.6×10^{-6} cc/sec. The leakage rate was about 40 percent less after the 50 cycles, which is an effect opposite to that experienced in the previous test. Variations of this order were noted throughout this series of tests, and were completely random. They are probably due to the seal being seated on a slightly different surface position on each hatch closing. Separate leakage tests were made on the window, pressure-equalization valve, and the actuation-shaft penetration. In each of these cases, no leakage was detectable with the present system.

Figure 25 presents the leakage of hatch B, which contained the molded type seal illustrated in figure 9, pressure loaded toward the closed position. Maximum measured leakage was 5.4×10^{-6} cc/sec after 1 cycle and 4.8×10^{-6} cc/sec after 50 cycles of hatch operation. The least leakage was noted after the 50 cycles. The leakage rate of the molded seal was approximately of the same order of magnitude as that for the O-ring seal in hatch A.

Figure 26 presents the leakage of hatch B pressure loaded toward the open position. Maximum measured leakage was 5.2×10^{-5} cc/sec after 1 cycle of operation and 1.4×10^{-5} cc/sec after 50 cycles of hatch operation. Leakage after 1 cycle of operation was almost 10 times greater for this test than when the hatch was loaded toward the closed position as shown in figure 25. After 50 cycles, the leakage also was several times that measured with the pressure loading toward the closed position. This effect can possibly be attributed to the unsymmetrical shape of the hatch B configuration. When loaded toward the open position, the hatch is being deflected away from the seal. Because the structure is not symmetrical, the hatch and hatch frame probably are not deflected uniformly at the seal seating surface. This condition is contrasted with that of hatch A where little difference was noted between leakage when the hatch was loaded toward the open and closed positions.

Figure 27 presents the leakage rate as a function of time for hatch B loaded toward the closed position. During this test leakage measurements were made over a period of 75 days, the hatch remaining closed during the entire time. The maximum measured leakage during this test was 2.8×10^{-5} cc/sec. Variations were noted from time to time. A mean line throughout the data indicates a stable leakage rate throughout the test. The cause of the variations from the mean line are not known. At the time of this test the same seal had been in use on the air lock for a period of over 2 years. No noticeable deterioration of the seal was detected during this time.

Figure 28 presents the leakage rate of hatch C, which contained the inflatable seal, the pressure forcing the hatch toward the closed position. Maximum measured leakage was 1.7×10^{-5} cc/sec after 1 cycle and 1.5×10^{-5} cc/sec after 50 cycles of hatch and seal opening. Leakage rates of the inflatable seal were generally greater than those for the O-ring seal on hatch A and for the molded seal on hatch B when forced toward the closed position. When the contoured surface on which this hatch had to seal is considered, this leakage rate is remarkably low. Initial leakage after 1 cycle was considerably lower than that after 50 cycles but the rates were nearly equal after 100 minutes. Cycling caused possible differences in the seating of the seal, and the associated leakage rates were probably due to the viscoelastic properties of the seal material.

Figure 29 presents the leakage rate of hatch C with pressure forcing the hatch toward the open position. Maximum measured leakage was 2.1×10^{-5} cc/sec after 1 cycle and 5.9×10^{-5} cc/sec after 50 cycles of operations. Leakage was somewhat higher when the hatch was loaded toward the open position compared with the results reported for the hatch loaded toward the closed position in figure 28. Leakage rates for the inflatable seal, although slightly higher than those for the other types of seals, are still less than 1 cc/day.

Higher Temperature Tests

The heat tests on the hatches were conducted by heating them to the desired temperature and then making leakage measurements. Cyclic tests were not performed because of the difficulty of removing and reinstalling the insulating blanket.

Figure 30 presents the leakage measured on hatch A with loading toward the closed position, at average seal interface temperatures of 150° F (66° C) and 201° F (93° C). The maximum measured leakage rate at 201° F (93° C) was 7.2×10^{-5} cc/sec, which was almost 5 to 10 times greater than that for tests at room temperature.

During the third higher temperature test on hatch A, the hatch failed structurally while being heated to 250° F (121° C). Leakage measurements had not been started at the time of failure; however, the interior of the air lock was under vacuum and the exterior at atmospheric pressure. Figure 31 shows the areas in which the metal skin parted from the honeycomb core. At the time of failure the seal continued to retain the vacuum inside the air lock. Further testing of hatch A was terminated after this damage. A possible cause of the failure may have been the pressure buildup from the bonded honeycomb sealed within the structure. The honeycomb was vented between cells but not vented to the outside of the structure.

Figure 32 shows the leakage rate of hatch B with the hatch at an average temperature of 142° F (60° C) and 193° F (89° C) and with the hatch pressure loaded toward the closed position. The maximum measured leakage was 1.7×10^{-5} cc/sec. The leakage

10

rate increased during the heating tests as observed during the heating tests on hatch A although the increase was not as great as that for hatch A.

Figure 33 shows the leakage rate of hatch C with the hatch at average temperatures of 150° F (66° C) and 177° F (81° C) and for the hatch pressure loaded toward the closed position. The maximum measured leakage was 2.4×10^{-6} cc/sec. Leakage for hatch C was almost an order of magnitude less during these tests than for tests at room temperature. This effect is exactly opposite to that which occurred on the O-ring seal on hatch A and the molded seal on hatch B. The reason for this lower leakage rate is not apparent and should be investigated further.

Lower Temperature Tests

Cold-temperature leak-rate tests were performed with the apparatus as previously described. Leakage measurements were started at the time cooling was started and continued for a period of 3 hours. Cyclic tests were not performed because of the difficulty of removing and reinstalling the insulating blanket. Since hatch A had failed structurally during heating tests, no cooling tests were conducted on this hatch.

Figure 34 presents the results of leakage measurements on hatch B during the cooling tests with the hatch pressure loaded toward the closed position. Figure 35 shows the average temperature of the structure on both sides of the seal as a function of time during the test. The maximum measured leakage was 9.7×10^{-4} cc/sec. Leakage rates increased rapidly when the temperature was lowered below 0° F (-18° C) but remained relatively constant between -10° F (-24° C) and -40° F (-40° C). The maximum measured leakage rate was $1\frac{1}{2}$ to $2\frac{1}{2}$ orders of magnitude higher than that previously measured for hatch B at room temperature. A subsequent test at a higher cooling rate caused the seal to unseat, and excessive leakage to occur. It was noted from the pressure gages that a possible unseating of the seal caused loss of vacuum in the system and made leakage measurements impossible with the present system. Increased leakage and seal unseating could have been caused by differential deflection of various parts of the unsymmetrical hatch and hatch frame during the cooling cycle.

Figure 36 presents leakage rate as a function of time for hatch C with the hatch pressure loaded toward the closed position for the cooling tests. The maximum measured leakage was 3.9×10^{-5} cc/sec. Figure 37 presents the average temperature on the structure on both sides of the seal as a function of time for the tests. During the cooling tests the maximum leakage rate was about twice that measured during the room-temperature tests. Some fluctuation of leakage during the test was noted, probably because of the shifting of the seal by contraction due to cooling. The good performance of this seal during cooling was not expected since butyl elastomer becomes hard at lower temperatures; however, the low leakage of the inflatable seal during the cooling tests may be due

to the ability to maintain a uniform seating stress on the seal even during structural deflections.

General Discussion

Several additional problems which were associated with the operation of air lock during the tests are described in this section.

Although no mechanical problems were associated with the use of molybdenum disilicide as a lubricant in a vacuum system (the wear surfaces remained lubricated during the entire series of tests), one unexpected problem occurred with the use of this lubricant. In the vacuum condition of 10^{-6} torr, molybdenum disilicide slowly migrated and deposited on all interior surfaces of the vacuum system. After a period of several weeks it shorted out the vacuum-measuring ionization gages and prevented use of the residual gas analyzer on the system. This slow migration of molybdenum disilicide may be desirable for continued lubrication of wearing parts but contamination of other parts is undesirable.

An additional problem was encountered with the pressure-equalization valves (fig. 4) which could not be opened by hand after being sealed for several days with a pressure differential across the valves of 1 atmosphere (1 atmosphere = 1×10^5 N/m^2). It was necessary in this case to insert a hammer handle or other means to provide additional leverage to open them. This problem could possibly be alleviated by making the valve seat smaller or by designing a different type of valve mechanism. Equalization time to reduce the pressure from 1 atmosphere to vacuum with the present valves was approximately 9 seconds. If this time were increased to approximately 1 minute, the valve seat would probably be small enough to be opened manually even after extended periods of time.

Information derived from the tests on this air lock may be of value in the design of future manned space vehicles. A lightweight air-lock system has been constructed and successfully tested under vacuum conditions to investigate leakage problems. Leakage rates attained during the tests were on the order of 10 cc or less per day, which would be almost negligible for atmospheric confinement. An acceptable leakage rate for long-term space use has been achieved; however, a number of problems arose during the tests which require additional research or which require special design consideration when air-lock structures are being designed. These problems include the structural failure of the honeycomb hatch and frame when being heated above 200° F (93° C), the unseating of the molded seal on hatch B due to uneven deflections, the migration of the molybdenum disilicide solid lubricant, and the excessive leverage required to open the pressure-equalization valves.

Of the three hatch configurations tested, the circular hatch A in the concentric hatch frame was less affected by loading direction and temperature changes than the oval-type

configuration. It appears that the contoured hatch C with the inflatable seal was best able to compensate for structural deflections. Future hatch designs where unequal structural deflections occur should be given special design consideration to prevent unseating of the seal. This unseating could be prevented by additional structural reinforcement in the area of the seal or design of the seal to tolerate greater structural deflections before unseating.

The mechanical actuation systems of the air lock operated reliably throughout this series of tests except for the problem of the sticking pressure-equalization valves mentioned previously. Each hatch was operated in excess of 100 times and continued to seal reliably.

Of the three types of seal configuration used, no seal failures due to deterioration were noted. After more than 2 years of use, the same seals continued to seal satisfactorily. Leakage rates did not vary greatly between one seal type and another; however, the leakage rate was affected by direction of loading of the hatch, deflection of the structure on which the seal was seated, and temperature. In the tests described in this paper, the inflatable seal appeared to be least affected by structural deflections.

CONCLUDING REMARKS

A lightweight air-lock structure has been successfully constructed and vacuum tested to determine structural sealing problems and leakage rates over a temperature range from -40° F $(-40^\circ$ C) to 200° F $(93^\circ$ C). Three different types of hatch configurations were tested, each having a different type of seal.

Leakage rates sufficiently low for manned space flight structures were attained during the tests. Leakage rates less than 10^{-4} cc/sec or less than 10 cc/day of helium were attained except in cases where the seal appeared to unseat in the case of the cooling tests. Leakage rates did not vary greatly between one seal type and another. Leakage rates tended to increase when the temperature was varied appreciably above or below room temperature. Loading of the hatches toward the open position tended to increase leakage rates. Opening and closing the hatches a large number of times did not appreciably affect the leakage rates.

The circular hatch was least affected by structural loading whereas the contoured hatch with the inflatable seal was probably best able to tolerate structural deflection. Leakage rates of the oval hatch configuration varied more with direction of loading and temperature variations.

It is recommended that problems of structural integrity of the honeycomb structure, uneven structural deflection, and leakage rates at lower temperatures be investigated in greater detail in future research.

Langley Research Center,
    National Aeronautics and Space Administration,
        Hampton, Va., June 8, 1970.

REFERENCES

1. Anon.: Space Station Connection and Seal Study. Contract NAS1-2164, Environmental Res. Associates (Randallstown, Md.), Oct. 1962.

2. Farkass, Imre; and Barry, Edward J.: Study of Sealants for Space Environment. NRC Res. Proj. No. 43-1-139 (Contract DA-19-020-506-ORD-5097), Nat. Res. Corp. (Cambridge, Mass.), 1960.

3. Mauri, R. E.: Seals and Gaskets. Space Materials Handbook, Clause G. Goetzel and John B. Singletary, eds., Contract AF 04(647)-673, Lockheed Missiles and Space Co., Jan. 1962, pp. 325-348.

4. Trout, Otto F., Jr.: Sealing Manned Spacecraft. Astronaut. Aerospace Eng., vol. 1, no. 7, Aug. 1963, pp. 44-46.

5. Anon.: Seals Reference Issue. Mach. Des., vol. 41, no. 14, June 19, 1969.

6. Trout, Otto, F., Jr.: Investigation of Man's Extravehicular Capability in Space by Water Immersion Simulation Techniques. Paper presented at AIAA Third Annual Meeting and Technical Display (Boston, Mass.), Nov.-Dec. 1966.

7. Loats, Harry L., Jr.; and Bruchey, William J., Jr.: A Study of the Performance of an Astronaut During Ingress and Egress Maneuvers Through Airlocks and Passageways. NASA CR-971, 1968.

8. Smith, E. A.: A Lunar Shelter Airlock. NSL 63-251, Northrop Space Lab., Sept. 1963.

9. Johnson, Sherwin F.; and Roberts, Edward O.: Crew Station Research for Aerospace Vehicles Experiments Performed Under Zero-Gravity. Part I: Translation and Hatchway Ingress-Egress Techniques. AFFDL-FDFR-TM-64-23, U.S. Air Force, 1963. (Available from DDC as AD 815029.)

10. Trout, Otto F., Jr.: An Investigation of Leakage of Large-Diameter O-Ring Seals on Spacecraft Air-Lock Hatches. NASA TN D-4394, 1968.

11. Schulte, L. O.: Airlock Experiment for Saturn S-IVB/SA 209, Rep. SM-51894P, Missile & Space Syst. Div., Douglas Aircraft Co., Inc., Mar. 7, 1966.

12. Dunkelberger, R. H.: Stress Analysis of NASA-Langley Airlock. Report No. 47724 (Contract No. NAS1-3893), Missile & Space Syst. Div., Douglas Aircraft Co., Inc., Sept. 1964.

13. Maintenance Manual Test Model Flight-Type Airlock. SM 48184 (Contract NAS1-3893), Missile & Space Syst. Div., Douglas Aircraft Co., Inc., [1964].

TABLE I.- AIR-LOCK MASS BREAKDOWN

	Mass	
	lb	kg
Primary structure:		
Assembly, 21-inch (0.53-meter) long cylinder	28	13
Assembly, 60-inch (1.53-meter) long cylinder	100	45
Hatch C, body assembly	26	12
Hatch A, assembly	51	23
Hatch A, frame assembly	56	25
Hatch B, assembly	60	27
Hatch B, frame assembly	56	25
Total air-lock mass	377	171
Auxiliary components not part of primary flight-weight structure:		
Adaptability flanges (nonflight weight)	63	28
Electronics and lighting system	34	15
Miscellaneous support bracketry	10	5
Total mass	107	48

TABLE II.- LEAKAGE MEASUREMENTS DURING ACCEPTANCE TESTS

Test setup	Maximum acceptable leakage per 24 hours, cc	Measured leakage per 24 hours, cc
21-inch (0.53-meter) cylinder	6.0	0.3
60-inch (1.53-meter) cylinder	10	.5
Hatch A, normal	100	.2
Hatch A, inverted	100	.5
Hatch B, normal	100	13.5
Hatch B, inverted	100	5.5
Hatch C, normal	100	17.3
Hatch C, inverted	100	.1

TABLE III.- SUMMARY OF AIR-LOCK LEAKAGE TESTS

Test	Hatch	Direction of pressure loading (a)	Temperature[b]		Maximum leakage rate, cc/sec
			°F	°C	
1	A	Closed (1 cycle)	Room		3.1×10^{-6}
2	A	Closed (50 cycles)	Room		1.0×10^{-5}
3	A	Open (1 cycle)	Room		6.2×10^{-6}
4	A	Open (50 cycles)	Room		2.6×10^{-6}
5	B	Closed (1 cycle)	Room		5.4×10^{-6}
6	B	Closed (50 cycles)	Room		4.8×10^{-6}
7	B	Open (1 cycle)	Room		5.2×10^{-5}
8	B	Open (50 cycles)	Room		1.4×10^{-5}
9	B	Closed (1 cycle)	Room		2.8×10^{-6}
10	C	Closed (1 cycle)	Room		1.7×10^{-5}
11	C	Closed (50 cycles)	Room		1.5×10^{-5}
12	C	Open (1 cycle)	Room		2.1×10^{-5}
13	C	Open (50 cycles)	Room		5.6×10^{-5}
14	A	Closed (1 cycle)	150	65	6.4×10^{-5}
15	A	Closed (1 cycle)	201	94	7.2×10^{-5}
16	B	Closed (1 cycle)	140	60	1.2×10^{-5}
17	B	Closed (1 cycle)	193	89	1.7×10^{-5}
18	C	Closed (1 cycle)	150	65	2.4×10^{-6}
19	C	Closed (1 cycle)	177	80	1.0×10^{-6}
20	B	Closed (1 cycle)	-48	-44	9.7×10^{-4}
21	B	Closed (1 cycle)	-39	-39	9.3×10^{-4}
22	C	Closed (1 cycle)	-34	-37	3.9×10^{-5}
23	C	Closed (1 cycle)	-44	-42	2.8×10^{-5}

aClosed, pressure loading forces hatch against seal; open, pressure loading forces hatch away from seal.

bRoom temperature is 75° F to 80° F (24° C to 27° C).

18
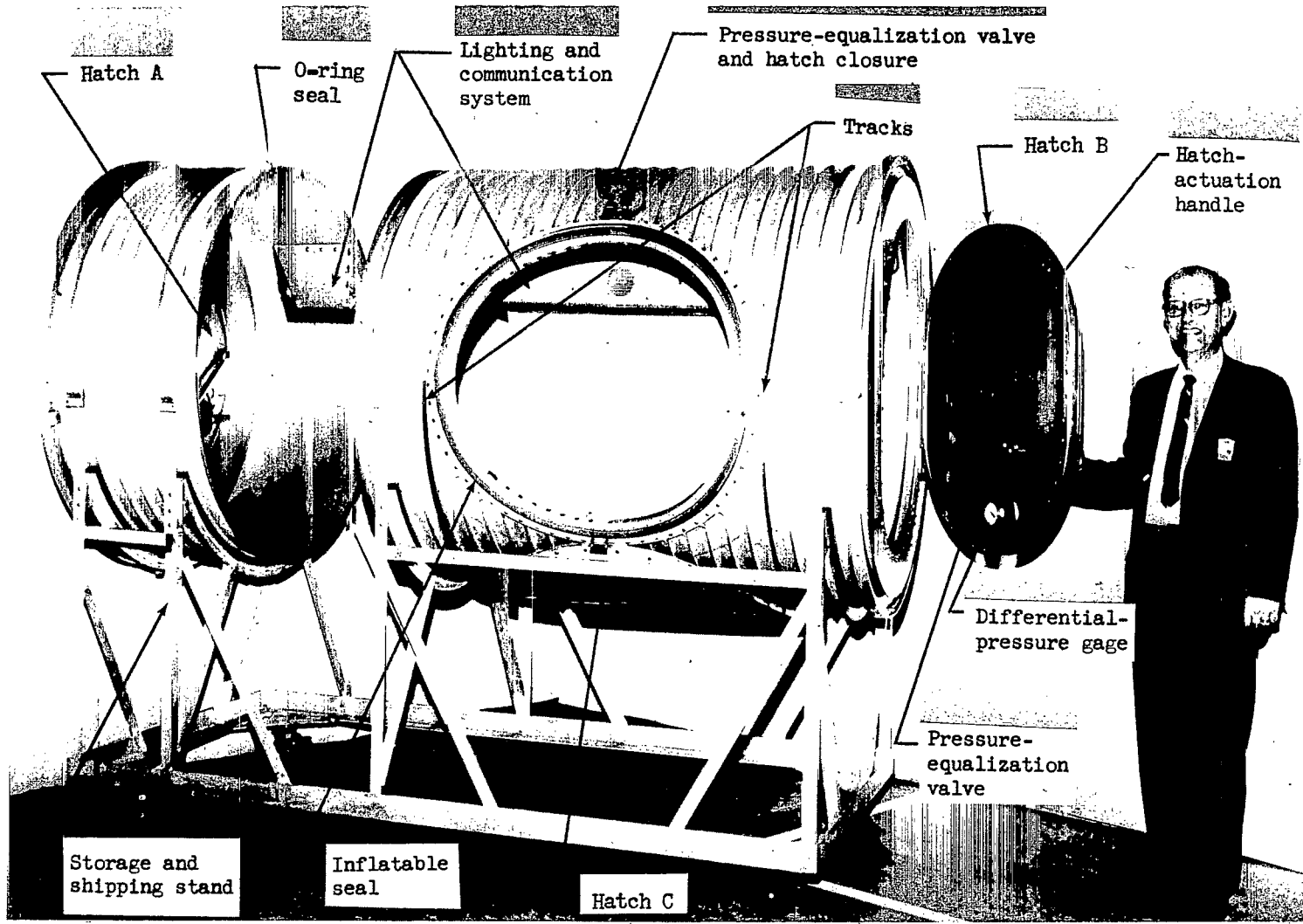
Figure 1.- Lightweight simulated spacecraft air lock.

L-66-5811

Figure 2.- Hatch A.

L-70-1655

O-ring groove

.235 in.
5.96 mm

.234 in.
5.94 mm

24°   Detail A

Cam rollers

.275 in.
6.98 mm

.005 in.
.127 mm

.003 in.
.076 mm

O-ring cross section

Latching handles

Honeycomb core

Rotating rim

Hardened steel striker plate

Honeycomb core

Hatch frame

O-rings

O-ring
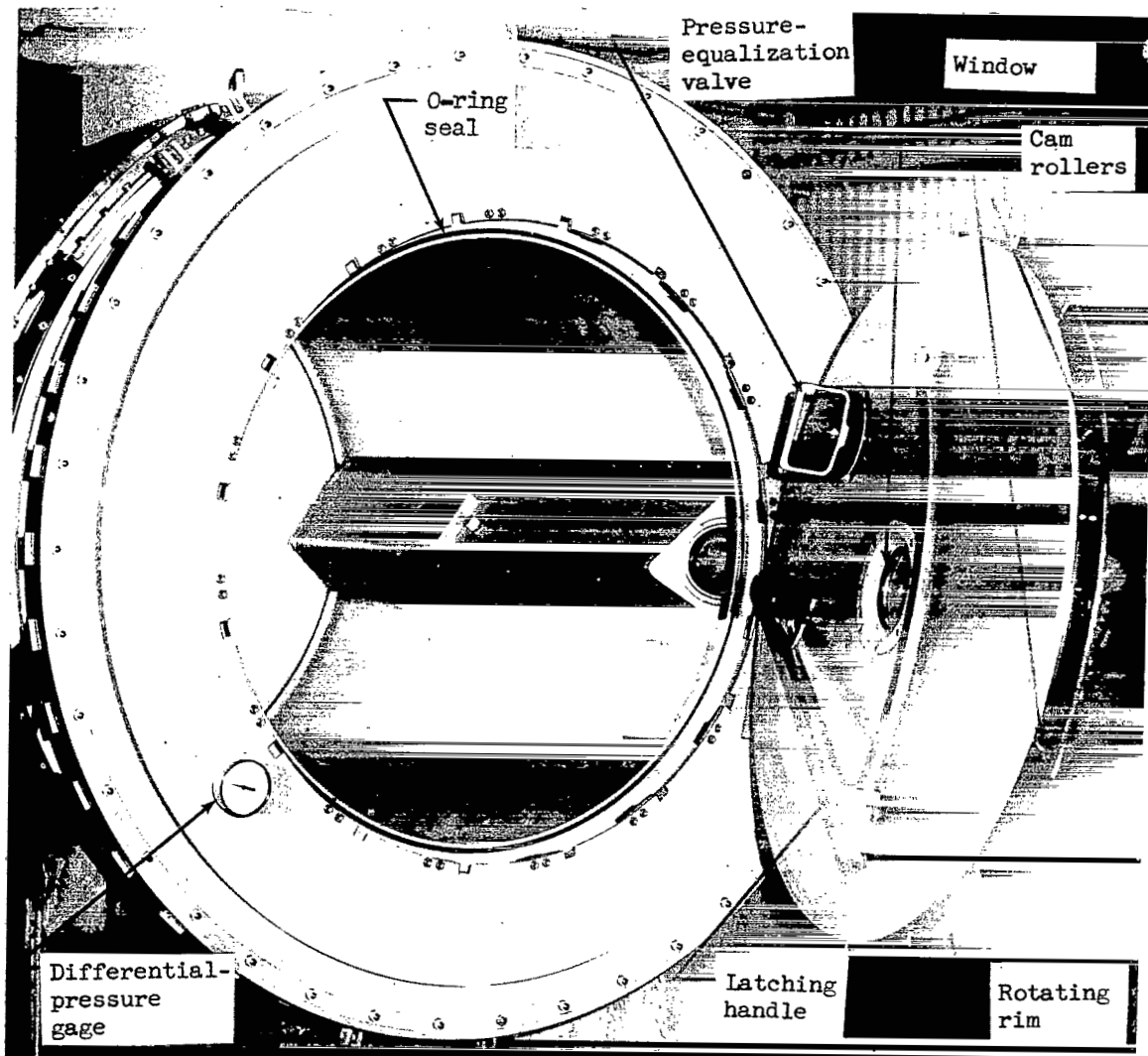
see detail A

Sectional view through hatch and frame.
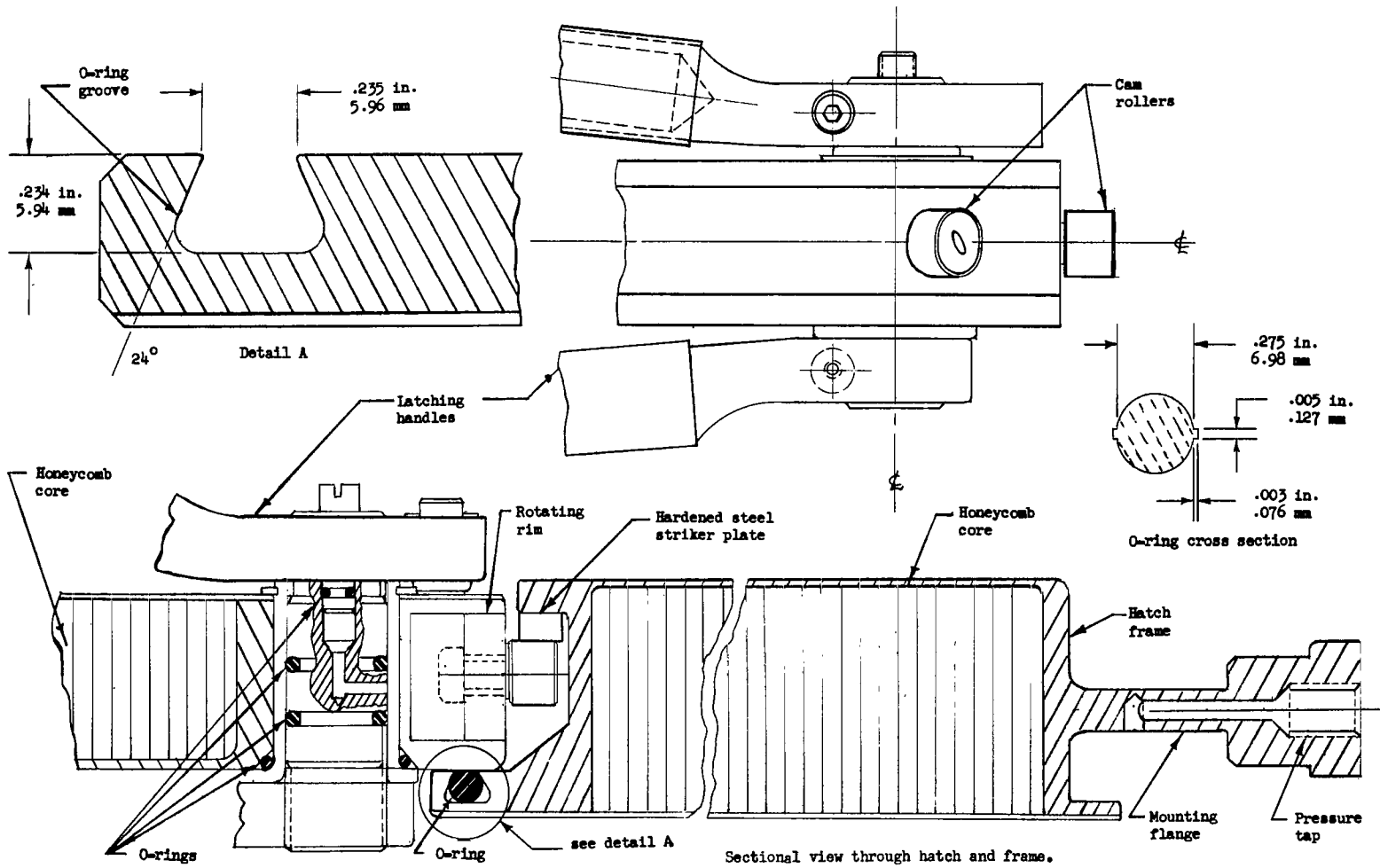
Mounting flange

Pressure tap

Figure 3.- Construction features of hatch A.

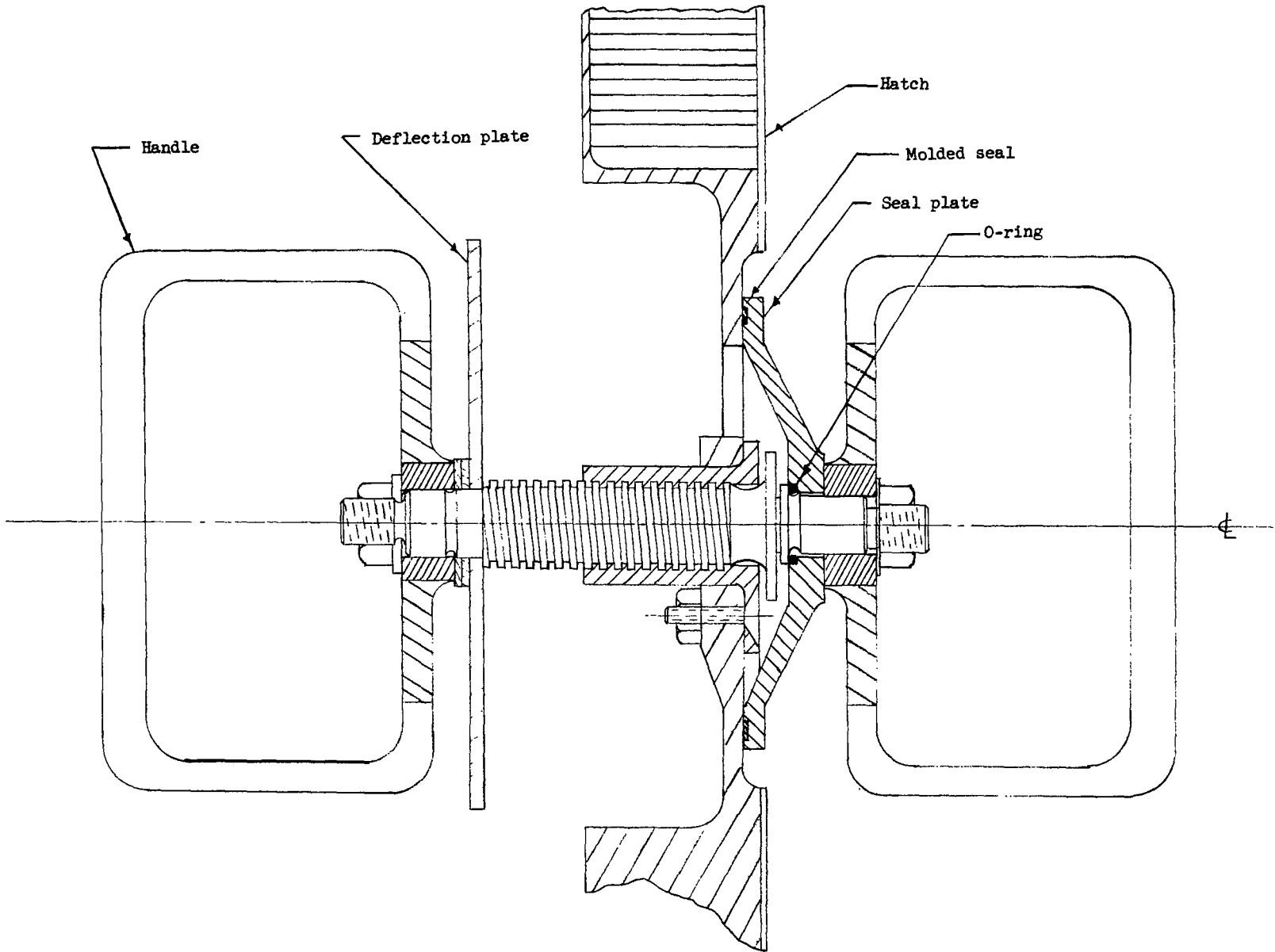Figure 4.- Pressure-equalization valve for hatch A and hatch B.
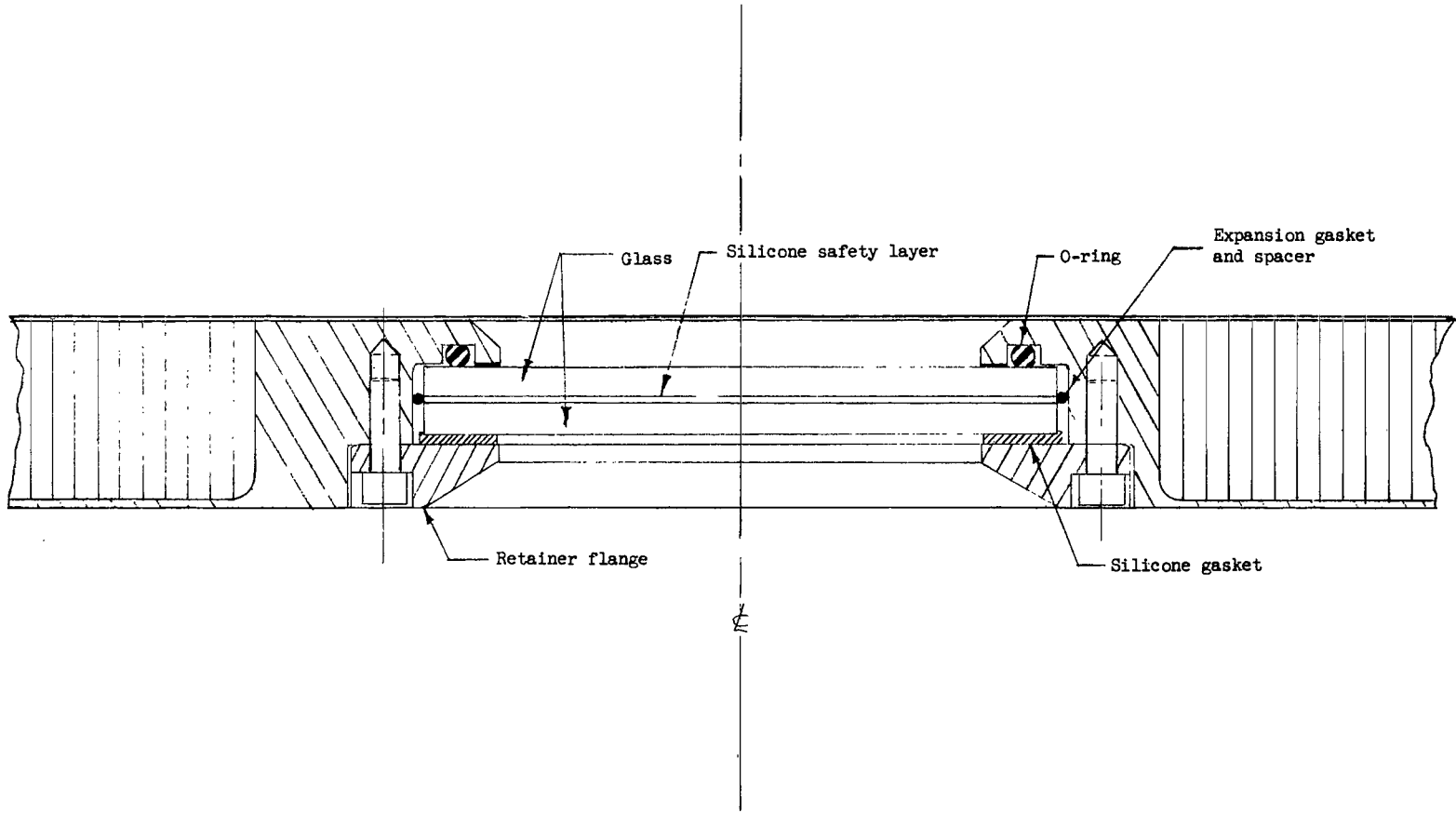
Figure 5.- Window in hatch A.

Labels in figure: Glass · Silicone safety layer · O-ring · Expansion gasket and spacer · Retainer flange · Silicone gasket

Airstream-
deflection
plate

Latching handle

Hinges

Pressure-equalization
valve

Differential-pressure
gage

L-70-1656

Figure 6.- Hatch B.

Rotary handle

Spiral plate

Push-pull actuation lever

Expander rings

Expander linkage

L-70-1657

Figure 7.- Latching mechanism in hatch B.
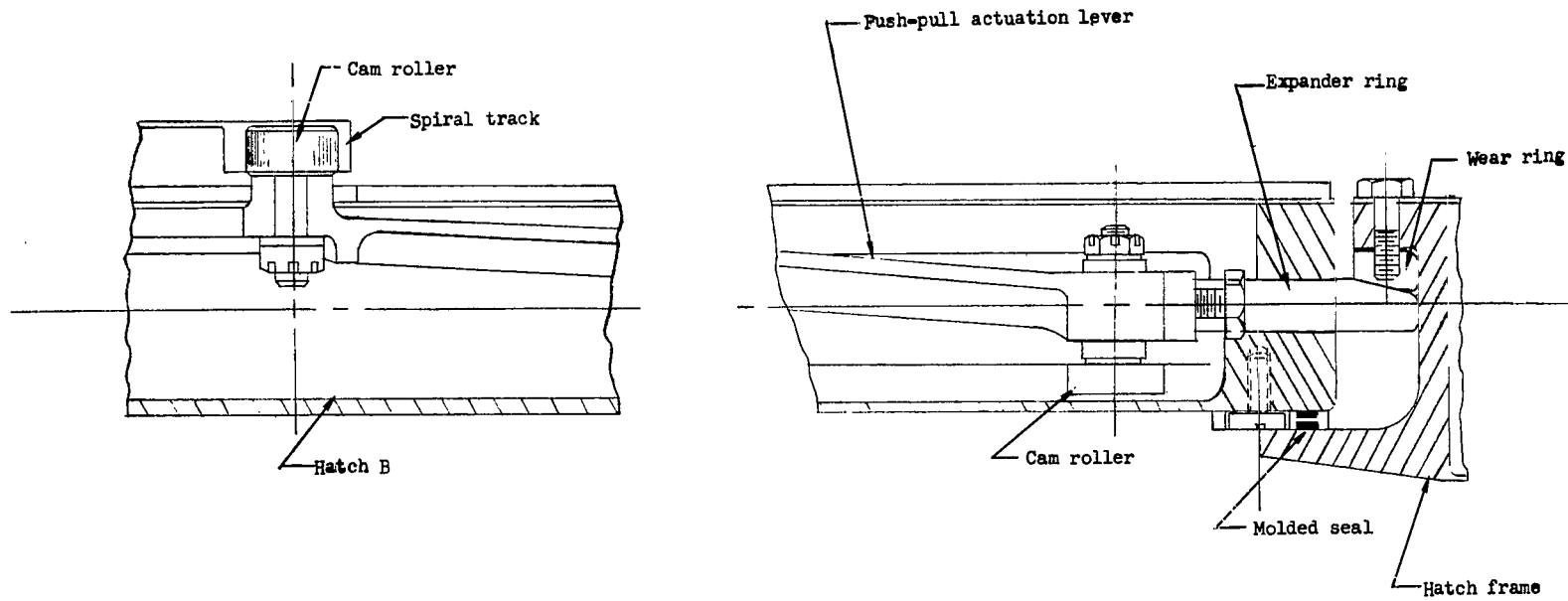
Figure 8.- Cross-sectional diagram of hatch B.
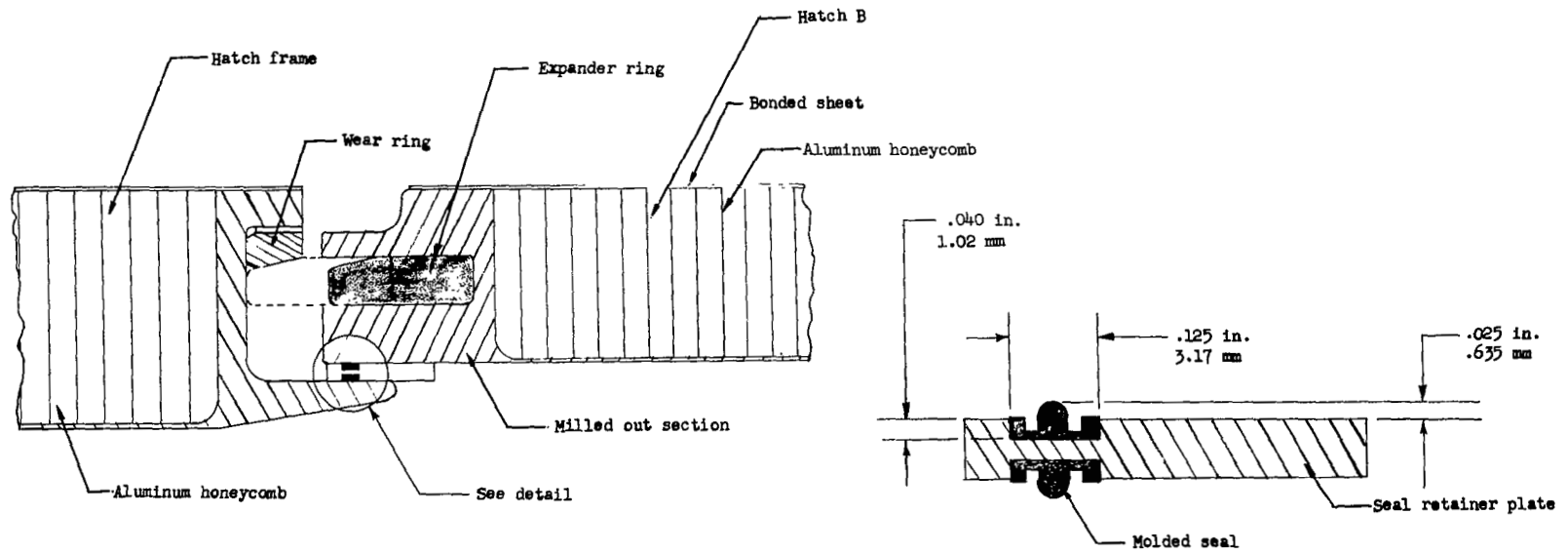
Figure 9.- Cross-sectional diagram of expander ring and molded seal.

Pressure-equalization valve and latching mechanism

Hatch C

Retainer lip

Track

Track

L-66-160

Figure 10.- Hatch C.
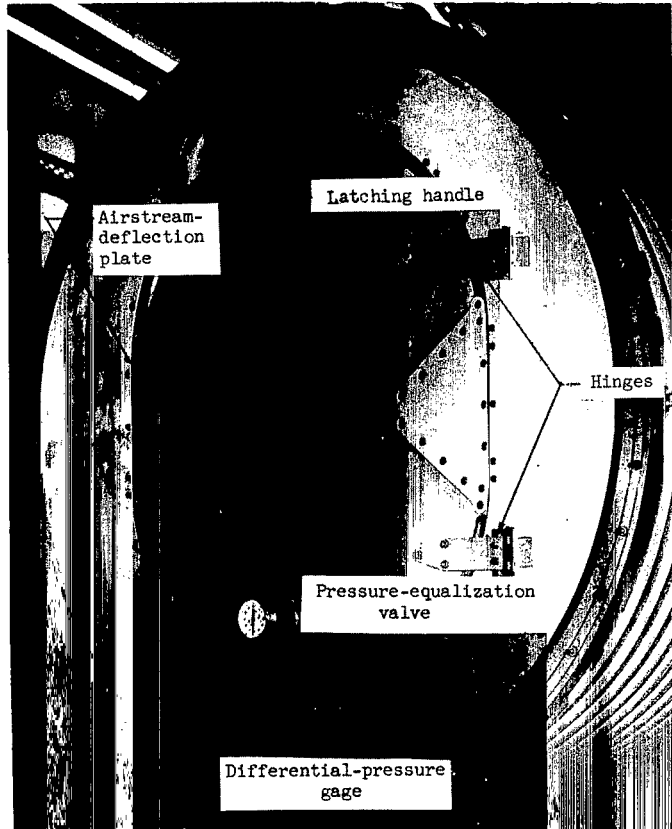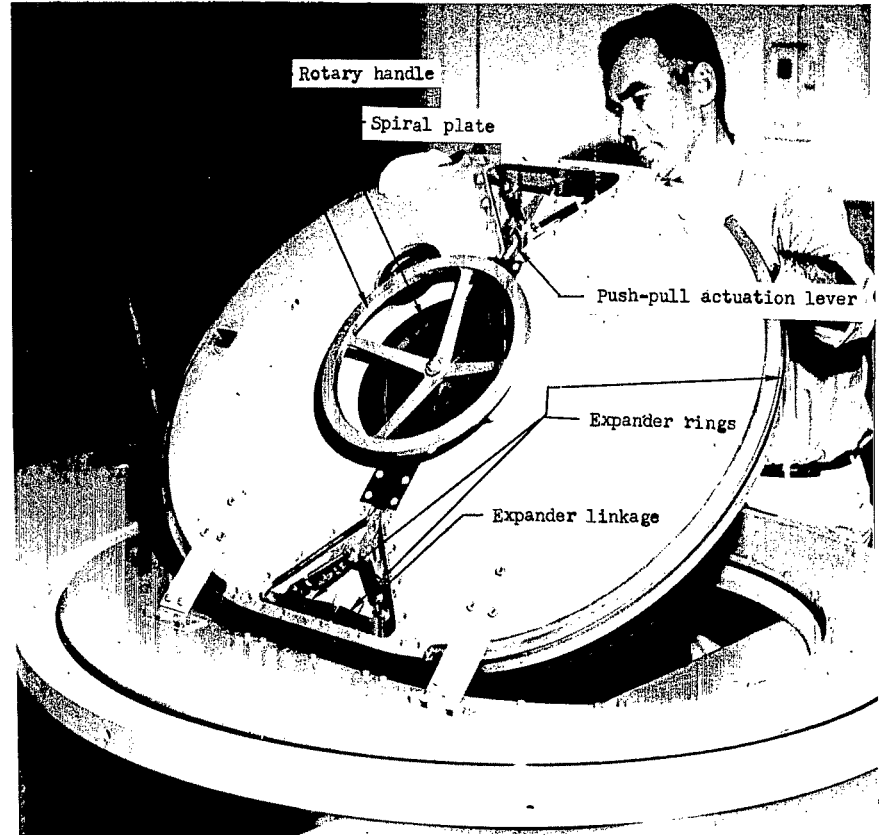
Bonded aluminum sheet

Aluminum honeycomb

Milled out section

Seal retainer ring

Hatch C

Hatch-latching mechanism

Hatch C

Track

Retainer lip

Inflatable seal

Retainer lip

Air-lock cylindrical section

Handle

Valve seal plate

Cross-sectional diagram of lower
side of hatch
(see figure 10.)

Cross-sectional diagram of upper
side of hatch
(see figure 10.)

Figure 11.- Cross-sectional diagram of the latching mechanism, inflatable seal, and pressure-equalization valve
for hatch C.
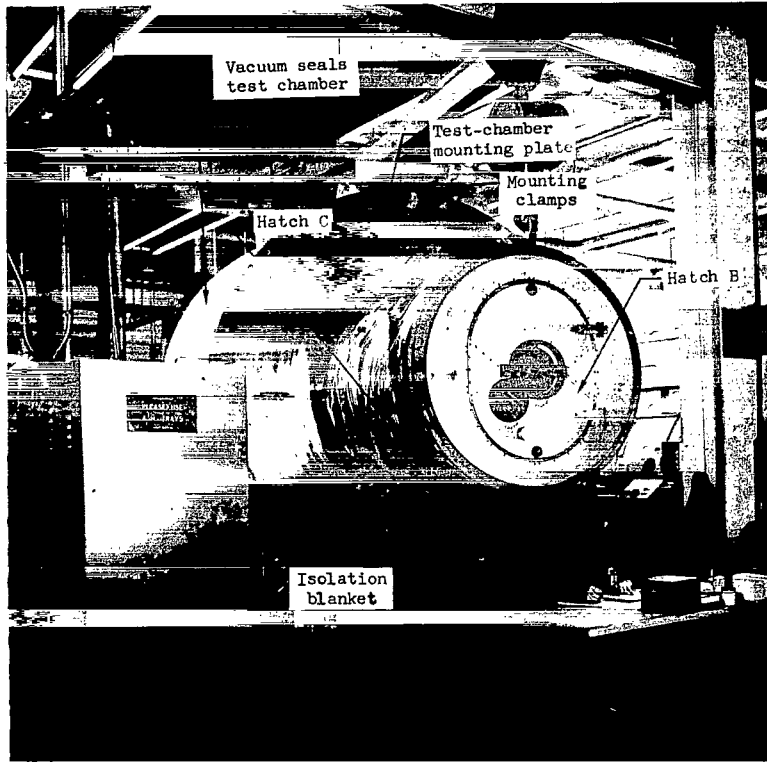
Figure 12.- The air lock mounted in the
seals test chamber.

L-66-159
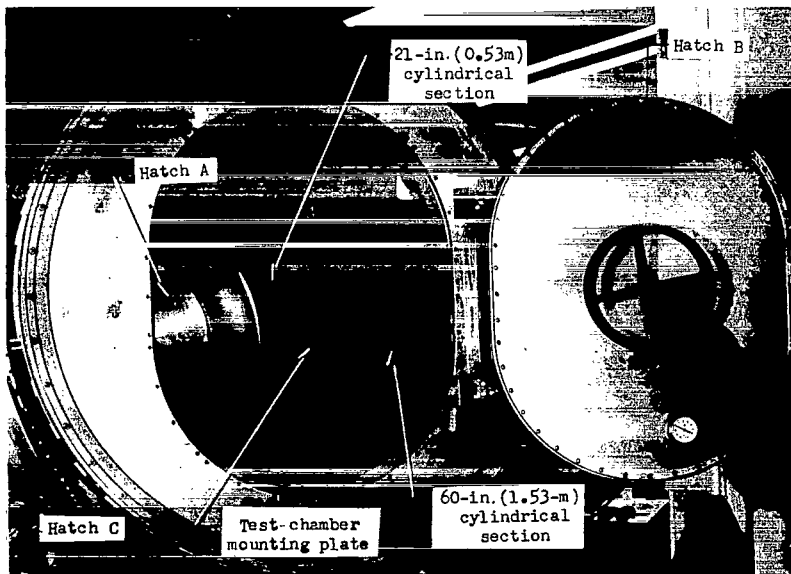
Figure 13.- The interior of the air lock mounted on the
test chamber.

L-70-1658

Helium inlet

Circumferential clamp

Helium outlet and to vacuum pump
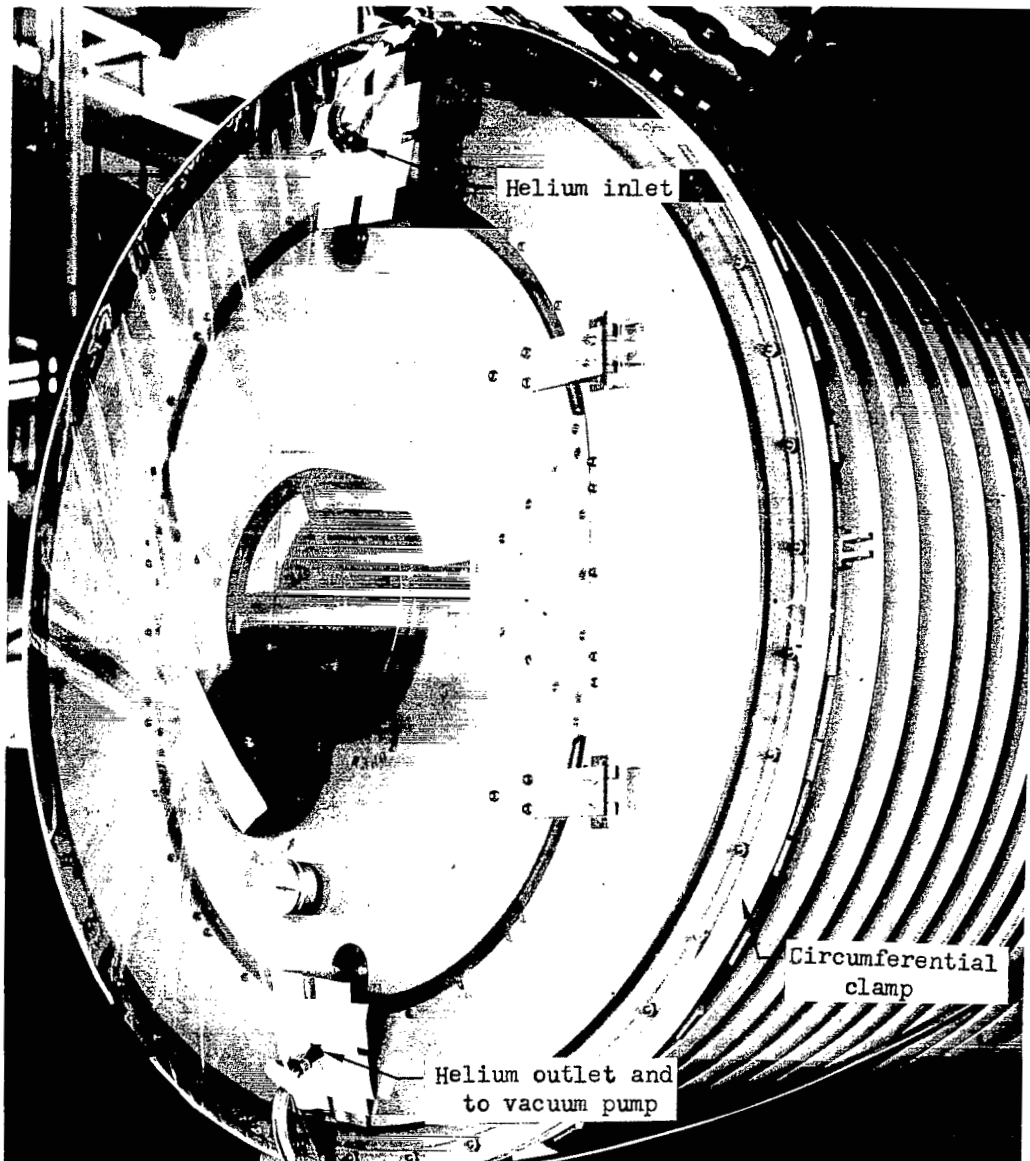
L-66-2785

Figure 14.- The helium isolation blanket installed on hatch B.
(Same arrangement as used on hatch A.)
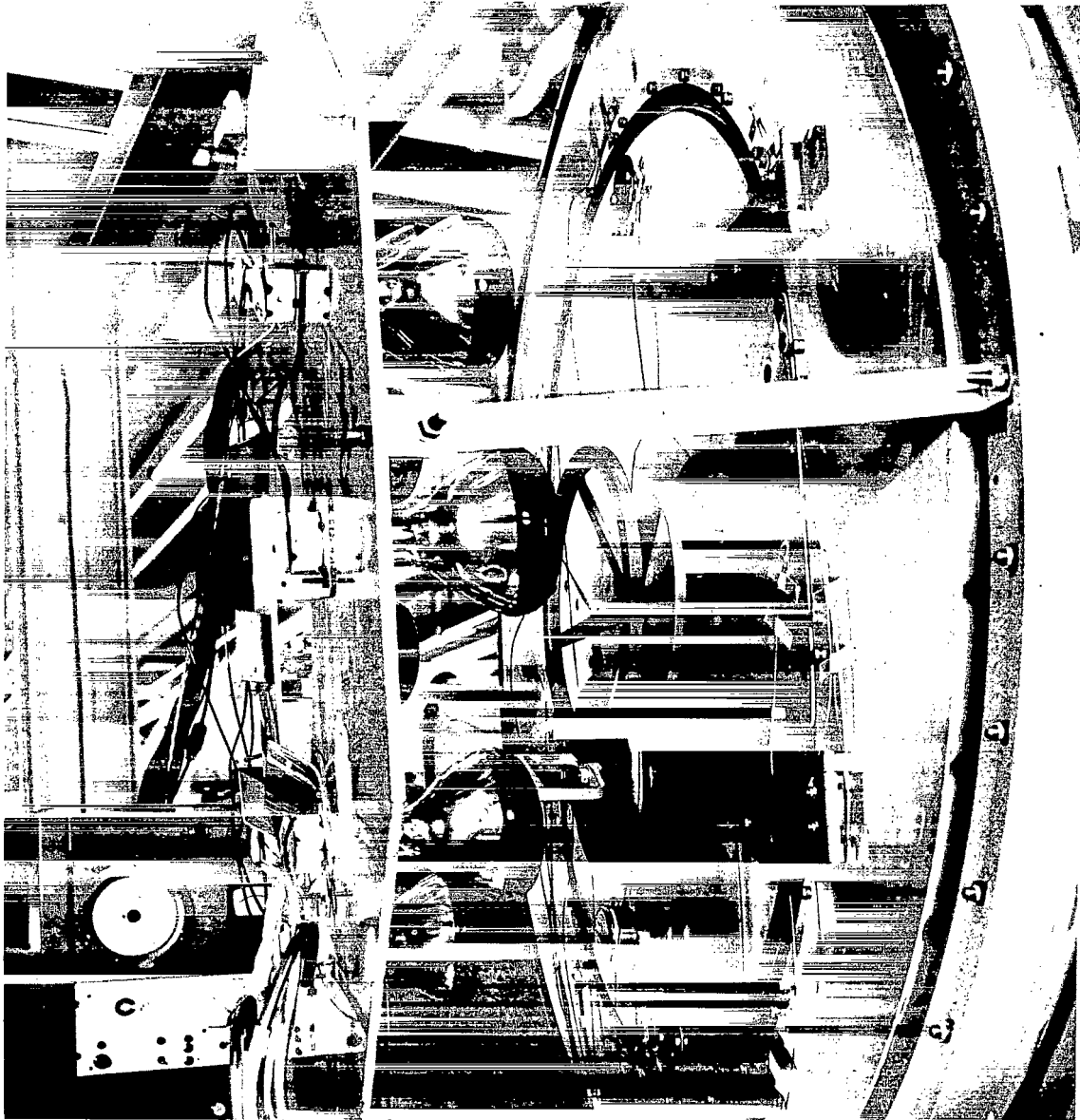
L-66-4117

Figure 15.- Arrangement of heat lamps for heating hatch B before installation of the insulating cover.

Table 3.- Continued.

(a) $C_{T,s} = 0.90$, $q_s = 20.24$

$\alpha = 65°$

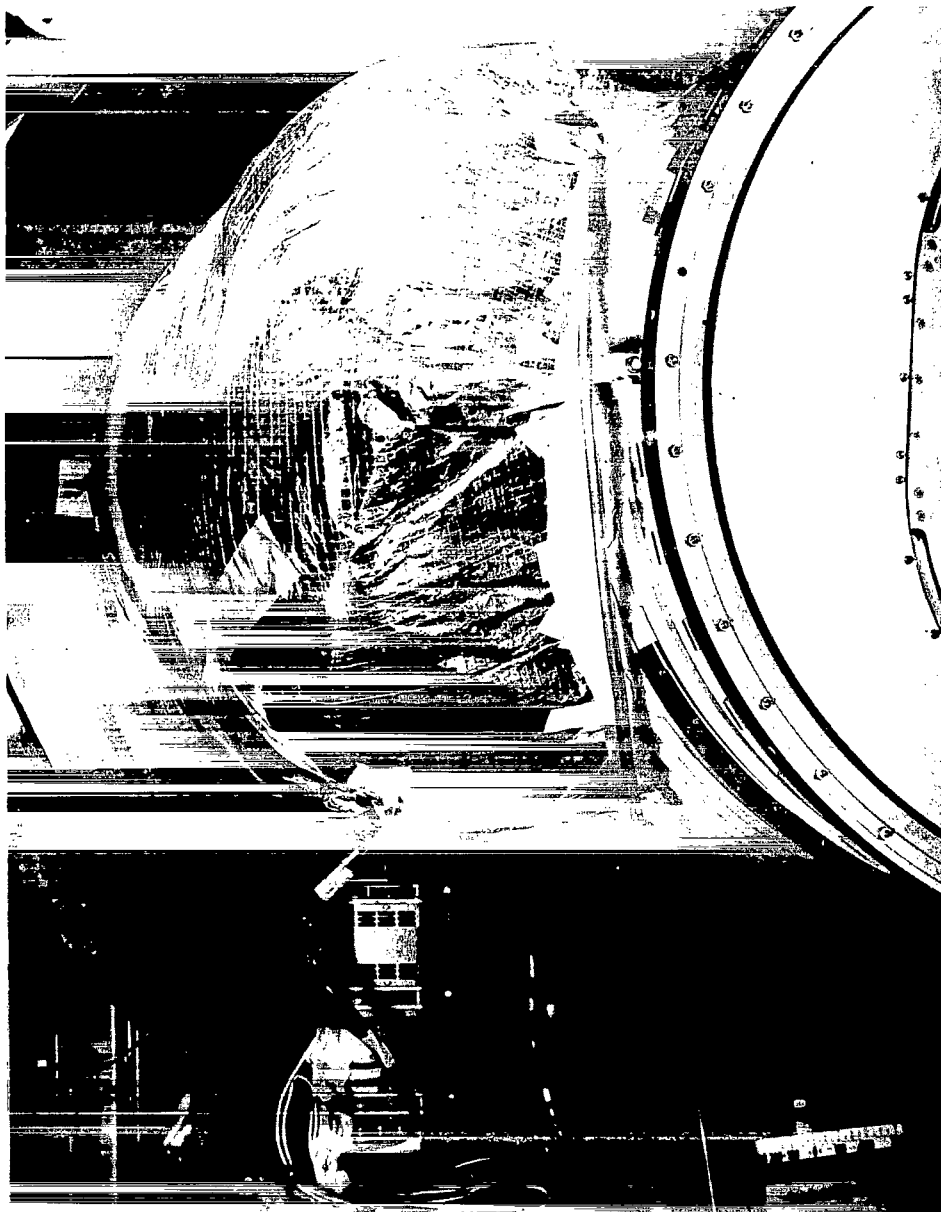| TUBE NO	1	2	3	4	5	6	7
1	.413	.785	.374	-3.415	-2.481	-1.839	-.489
2	.042	-.003	.012	-3.418	-2.973	-2.202	-.319
3	-.204	-.309	-.274	-2.864	-2.849	-1.882	-.359
4	-.621	-.742	-.450	-1.299	-2.446	-1.072	-.310
5	-.929	-1.058	-.726	-.760	-1.524	-.637	-.282
6	-000.000	-000.000	-000.000	-000.000	-000.000	-000.000	-000.000
7	-000.000	-000.000	-000.000	-000.000	-000.000	-000.000	-000.000
8	-000.000	-000.000	-000.000	-000.000	-000.000	-000.000	-000.000
9	-000.000	-000.000	-000.000	-000.000	-000.000	-000.000	-000.000
10	-.477	-1.022	-.845	-.507	-.554	-.303	-.245
11	-.971	-1.161	-000.000	-.417	-.365	-.222	-.283
12	-.793	-.875	-.524	-.130	-.384	-.247	-.290
13	-1.003	-.933	-.503	-.273	-.215	-.238	-.294
14	-1.221	-1.079	-.643	-.282	-.264	-.273	-.334
15	-.348	-.497	.226	.476	.376	.418	-.086
16	-.384	-.144	.138	.256	.192	.089	-.213
17	-1.153	-1.148	-.493	-.172	-.206	-.038	-.216
18	-1.401	-1.835	-1.079	-.430	-.392	-.379	-.382
19	-2.605	-2.549	-1.541	-.530	-.430	-.410	-.564
20	-2.766	-2.634	-1.306	-.414	-.341	-.199	-.299
21	-2.022	-2.265	-1.202	-.373	-.373	-.244	-.291
22	-2.186	-1.765	-.947	-.300	-.313	-.233	-.285
23	-1.957	-.828	-.499	-.284	-.283	-.252	-.240
24	-.714	-.127	-.148	-.196	-.124	-.109	-.166
25	.693	1.104	.872	-1.099	-.609	-.625	-.901
26	.284	.749	.834	.581	-000.000	-.372	-.140
27	-.402	-.147	.339	.631	.909	.472	.102
28	-.271	.023	.147	.711	.537	.222	.030
29	-.254	.246	.432	.513	.418	.376	.166
30	.593	1.040	.930	.853	.692	.780	-.175
31	.046	1.041	.994	.784	.810	.865	.001
32	.245	.748	.741	.685	.617	.679	.302
33	.025	.444	.514	.454	.343	.291	.150

$\alpha = 70°$

TUBE NO	1	2	3	4	5	6	7
1	.750	.741	.468	-2.182	-1.937	-1.704	-.469
2	.011	-.053	.122	-2.534	-2.796	-1.900	-.192
3	-.292	-.420	-.289	-2.633	-3.032	-1.646	-.180
4	-.685	-.797	-.366	-1.244	-2.446	-.703	-.341
5	-1.013	-1.134	-.618	-.577	-1.892	-.416	-.109
6	-000.000	-000.000	-000.000	-000.000	-000.000	-000.000	-000.000
7	-000.000	-000.000	-000.000	-000.000	-000.000	-000.000	-000.000
8	-000.000	-000.000	-000.000	-000.000	-000.000	-000.000	-000.000
9	-000.000	-000.000	-000.000	-000.000	-000.000	-000.000	-000.000
10	-.995	-1.071	-.872	-.492	-.456	-.236	-.193
11	-.960	-1.020	-000.000	-.354	-.327	-.247	-.129
12	-.679	-.815	-.457	-.105	-.374	-.262	-.299
13	-1.075	-.953	-.491	-.120	-.343	-.219	-.241
14	-1.197	-.933	-.434	-.240	-.312	-.217	-.244
15	-.386	-.936	.341	.425	.315	.394	-.242
16	-.378	-.067	.149	.274	.174	.051	-.131
17	-1.046	-1.038	-.354	-.090	-.279	-.059	-.115
18	-1.777	-1.732	-1.013	-.463	-.409	-.254	-.316
19	-2.406	-2.235	-1.245	-.430	-.517	-.252	-.323
20	-2.549	-2.089	-1.054	-.329	-.425	-.372	-.340
21	-2.476	-1.959	-1.060	-.354	-.361	-.239	-.403
22	-2.010	-1.577	-.864	-.315	-.295	-.330	-.410
23	-.999	-.591	-.315	-.217	-.172	-.170	-.252
24	-.712	-.135	-.204	-.193	-.157	-.169	-.163
25	.659	1.122	.732	-1.066	-.431	-.762	-.633
26	.160	.603	.847	.693	-000.000	.390	-.177
27	-.445	.164	.290	.703	.820	.358	.059
28	-.308	-.003	.150	.639	.462	.214	-.059
29	-.277	.241	.399	.519	.357	.213	.057
30	.545	1.046	.918	.896	.643	.480	-.116
31	.570	1.027	.778	.754	.742	-.134	
32	.311	.649	.715	.626	.558	.600	.354
33	.035	.465	.519	.436	.349	.268	.152

$\alpha = 75°$

TUBE NO	1	2	3	4	5	6	7
1	.668	.733	.262	-2.768	-1.999	-1.579	-.133
2	-.047	-.049	-.044	-2.414	-2.479	-1.412	-.147
3	-.292	-.378	-.198	-2.285	-2.799	-1.354	-.174
4	-.748	-.762	-.344	-1.407	-2.203	-.539	-.039
5	-1.080	-1.042	-.724	-.716	-1.404	-.286	-.067
6	-000.000	-000.000	-000.000	-000.000	-000.000	-000.000	-000.000
7	-000.000	-000.000	-000.000	-000.000	-000.000	-000.000	-000.000
8	-000.000	-000.000	-000.000	-000.000	-000.000	-000.000	-000.000
9	-000.000	-000.000	-000.000	-000.000	-000.000	-000.000	-000.000
10	-1.000	-1.040	-.757	-.380	-.348	-.140	-.050
11	-1.100	-1.142	-000.000	-.323	-.277	-.061	-.151
12	-.736	-.849	-.430	-.080	-.293	-.187	-.172
13	-1.097	-.894	-.462	-.242	-.234	-.204	-.293
14	-1.143	-.921	-.457	-.217	-.246	-.082	-.016
15	-.340	-.841	.270	.429	.341	.371	-.128
16	-.351	-.070	.214	.353	.245	.272	.041
17	-1.159	-1.082	-.341	-.030	-.164	-.031	-.005
18	-1.773	-1.599	-.922	-.334	-.336	-.302	-.185
19	-2.476	-2.223	-1.255	-.407	-.416	-.289	-.375
20	-2.516	-2.136	-1.175	-.373	-.290	-.122	-.326
21	-2.412	-1.918	-.942	-.313	-.278	-.177	-.245
22	-1.962	-1.591	-.850	-.282	-.182	-.159	-.240
23	-.973	-.575	-.354	-.221	-.209	-.131	-.087
24	-.419	-.144	-.276	-.141	-.140	-.176	-.171
25	.789	1.146	.610	-1.048	-.222	-.859	-.542
26	.210	.633	.716	.756	-000.000	.176	-.027
27	-.425	.173	.361	.752	.803	.411	.093
28	-.323	.021	.175	.643	.507	.248	.083
29	-.241	.256	.411	.528	.355	.197	-.037
30	.649	1.113	.915	.977	.687	.553	-.095
31	.669	1.047	.919	.904	.787	.779	-.052
32	.234	.742	.756	.606	.566	.644	.226
33	.253	.452	.565	.441	.347	.244	.161

$\alpha = 80°$

TUBE NO	1	2	3	4	5	6	7
1	.652	.739	.264	-3.116	-2.293	-1.816	-.461
2	-.057	-.033	-.093	-3.320	-2.692	-1.523	-.303
3	-.417	-.420	-.271	-3.570	-3.116	-1.251	-.119
4	-2.768	-2.594	-.707	-3.332	-2.819	-1.188	-.349
5	-1.093	-1.196	-.596	-1.661	-1.557	-.274	-.234
6	-000.000	-000.000	-000.000	-000.000	-000.000	-000.000	-000.000
7	-000.000	-000.000	-000.000	-000.000	-000.000	-000.000	-000.000
8	-000.000	-000.000	-000.000	-000.000	-000.000	-000.000	-000.000
9	-000.000	-000.000	-000.000	-000.000	-000.000	-000.000	-000.000
10	-1.102	-1.041	-.790	-.346	-.468	-.276	-.254
11	-1.158	-1.219	-000.000	-.339	-.456	-.178	-.263
12	-.755	-.859	-.497	-.010	-.213	-.178	-.179
13	-1.076	-.970	-.550	-.336	-.297	-.187	-.210
14	-1.097	-.935	-.479	-.232	-.252	-.096	-.249
15	-.347	-.907	.237	.435	.338	.346	-.191
16	-.405	-.091	.120	.248	.153	.130	-.074
17	-1.039	-.967	-.377	-.111	-.235	-.160	-.356
18	-1.739	-1.795	-1.045	-.524	-.424	-.338	-.294
19	-2.634	-2.432	-1.599	-.630	-.502	-.377	-.344
20	-2.655	-2.235	-1.253	-.391	-.411	-.419	-.497
21	-2.350	-1.954	-.905	-.293	-.286	-.173	-.249
22	-1.062	-1.447	-.697	-.187	-.267	-.202	-.210
23	-.829	-.013	-.517	-.258	-.292	-.295	-.257
24	-.708	-.111	-.127	-.215	-.285	-.275	-.331
25	.548	1.046	.717	-1.115	-.188	-.932	-.477
26	.207	.785	.744	.632	-000.000	.138	-.283
27	-.563	-.128	.255	.633	.764	.141	-.181
28	-.340	-.014	.131	.644	.421	.140	.041
29	-.351	.242	.354	.543	.312	.180	.099
30	.499	.851	.851	.834	.551	.420	-.079
31	.557	1.073	.996	.814	.686	.558	-.051
32	.235	.716	.677	.570	.537	.494	.194
33	.026	.468	.545	.437	.306	.191	-.054

32

L-67-1618

Figure 18.- Arrangement for heating hatch C.
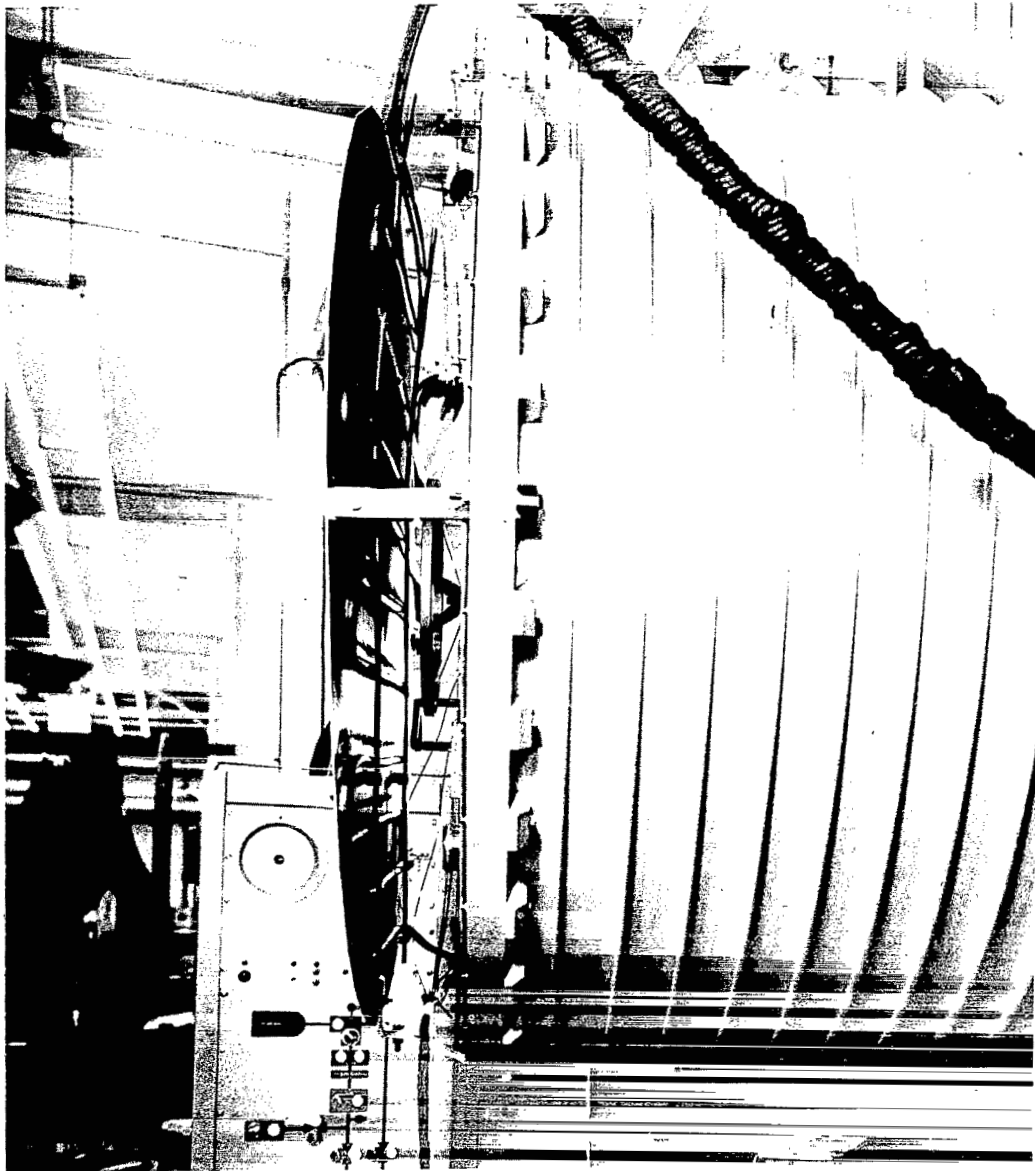
L-66-9189

Figure 19.- Arrangement of the coils for cooling hatch B before
enclosing hatch in the insulating cover.

L-66-9188

Figure 20.- Arrangement for cooling hatch B.

Table 3.- Continued.

(c) $C_{T,s} = 0.60$, $q_s = 21.67$

$\alpha = 5°$

TUBE NO	WING STATIONS						
	1	2	3	4	5	6	7
1	1.156	1.231	.691	-.278	.031	.387	.367
2	.733	.916	.455	-1.125	-.699	-.460	-.311
3	.662	.743	.368	-1.488	-1.271	-.693	-.502
4	.270	.307	.047	-1.426	-1.449	-1.117	-.821
5	-.174	-.184	-.327	-1.507	-1.700	-1.421	-1.079
6	*000.000	*000.000	*000.000	*000.000	*000.000	*000.000	*000.000
7	*000.000	*000.000	*000.000	*000.000	*000.000	*000.000	*000.000
8	*000.000	*000.000	*000.000	*000.000	*000.000	*000.000	*000.000
9	*000.000	*000.000	*000.000	*000.000	*000.000	*000.000	*000.000
10	-.499	-.521	-.760	-1.152	-1.132	-.919	-.601
11	-.617	-.692	*000.000	-1.032	-1.260	-1.028	-.834
12	-1.014	-.796	-.752	-.578	-1.000	-.787	-.617
13	-.516	-.721	-.672	-.653	-.828	-.688	-.444
14	-.593	-.720	-.631	-.674	-.822	-.680	-.493
15	-.057	.219	.357	.332	.316	.340	-.073
16	.069	-.011	.076	.110	.043	.037	-.058
17	-.438	-.642	-.399	-.475	-.776	-.529	-.441
18	-1.176	-1.285	-.948	-1.186	-1.426	-1.405	-.850
19	-1.543	-1.694	-1.481	-1.592	-1.887	-1.678	-1.061
20	-1.695	-1.692	-1.591	-1.599	-1.838	-1.822	-1.295
21	-1.892	-1.376	-1.225	-1.280	-1.540	-1.510	-1.133
22	-1.396	-.366	-.561	-.638	-.990	-1.210	-1.001
23	-.759	-.243	-.145	-.286	-.243	-.454	-.771
24	-.658	-.211	-.219	-.103	-.175	-.128	-.340
25	.473	.492	.244	.341	1.064	1.077	.869
26	-.269	-.344	.011	.391	*000.000	.876	.740
27	-.492	-.416	-.040	.519	.482	.367	.348
28	-.219	-.105	.160	.431	.311	.250	.242
29	.059	.260	.336	.392	.454	.443	.386
30	.671	1.046	.573	.901	.964	.969	.131
31	.906	1.039	.552	.911	.998	1.004	.760
32	.552	.692	.573	.949	.799	.785	.789
33	.744	.661	.451	.552	.561	.533	.050

$\alpha = 10°$

TUBE NO	WING STATIONS						
	1	2	3	4	5	6	7
1	1.079	1.043	.255	-1.339	-.736	-.248	-.237
2	.662	.670	.197	-1.989	-1.695	-1.316	-1.151
3	.423	.343	-.025	-2.221	-2.258	-1.505	-1.261
4	-.057	-.151	-.472	-2.221	-2.140	-1.791	-1.521
5	-.355	-.561	-.674	-2.143	-2.294	-1.872	-1.549
6	*000.000	*000.000	*000.000	*000.000	*000.000	*000.000	*000.000
7	*000.000	*000.000	*000.000	*000.000	*000.000	*000.000	*000.000
8	*000.000	*000.000	*000.000	*000.000	*000.000	*000.000	*000.000
9	*000.000	*000.000	*000.000	*000.000	*000.000	*000.000	*000.000
10	-.577	-.460	-.996	-1.543	-1.302	-1.149	-.949
11	*000.000	*000.000	*000.000	-1.206	-1.463	-1.187	-.991
12	-1.116	-.951	-.829	-.649	-1.065	-.822	-.682
13	-.556	-.797	-.725	-.694	-.864	-.737	-.550
14	-.651	-.795	-.691	-.682	-.648	-.688	-.696
15	-.004	-.091	.340	.362	.345	.396	-.155
16	.004	-.053	.107	.096	.022	.049	-.116
17	-.008	-.168	-.409	-.543	-.815	-.558	-.517
18	-1.133	-.943	-.966	-1.066	-1.500	-1.263	-.953
19	-1.747	-1.455	-1.542	-1.568	-1.831	-1.685	-1.244
20	-2.143	-1.633	-1.693	-1.658	-1.927	-1.992	-1.550
21	-1.843	-1.586	-1.643	-1.229	-1.463	-1.432	-1.200
22	-1.655	-1.037	-.748	-.847	-1.073	-1.247	-1.200
23	-1.026	-.254	-.225	-.205	-.259	-.353	-.899
24	-.652	-.206	-.265	-.094	-.114	-.099	-.332
25	.410	.436	.330	-.206	.658	.948	.745
26	.140	.199	.459	.631	*000.000	1.157	.902
27	-.251	-.158	.145	.631	.793	.716	.507
28	-.125	-.045	.248	.624	.442	.411	-.267
29	.113	.322	.410	.574	.524	.518	.384
30	.671	1.073	.625	.952	.951	1.005	.091
31	.990	1.152	.638	1.006	1.041	1.118	.722
32	.602	.769	.648	.826	.841	.828	.831
33	.521	.495	.470	.584	.560	.560	-.051

$\alpha = 15°$

TUBE NO	WING STATIONS						
	1	2	3	4	5	6	7
1	.946	.990	.029	-3.086	-2.097	-1.255	-1.082
2	.327	.193	-.343	-3.825	-3.068	-2.382	-1.955
3	.109	-.063	-.547	-3.948	-3.528	-2.662	-2.199
4	-.306	-.521	-.879	-3.642	-3.223	-2.718	-2.308
5	-.703	-1.017	-1.111	-2.821	-2.931	-2.619	-2.175
6	*000.000	*000.000	*000.000	*000.000	*000.000	*000.000	*000.000
7	*000.000	*000.000	*000.000	*000.000	*000.000	*000.000	*000.000
8	*000.000	*000.000	*000.000	*000.000	*000.000	*000.000	*000.000
9	*000.000	*000.000	*000.000	*000.000	*000.000	*000.000	*000.000
10	-.771	-1.145	-1.194	-1.893	-1.691	-1.617	-1.279
11	-.836	-1.255	*000.000	-1.391	-1.654	-1.454	-1.183
12	-1.229	-.932	-.898	-.693	-1.053	-.921	-.713
13	-.762	-.941	-.811	-.749	-.893	-.832	-.587
14	-.825	-.876	-.733	-.723	-.797	-.736	-.586
15	-.069	-.029	.434	.469	.426	.368	-.145
16	-.146	-.070	.103	.108	.040	-.049	-.147
17	-.075	-1.051	-.611	-.609	-.835	-.673	-.605
18	-1.551	-1.652	-1.239	-1.134	-1.378	-1.510	-1.136
19	-2.000	-1.960	-1.657	-1.288	-1.646	-1.548	-1.171
20	-2.443	-2.222	-1.748	-1.378	-1.597	-1.805	-1.483
21	-2.620	-2.059	-1.592	-1.132	-1.442	-1.623	-1.295
22	-2.237	-1.401	-1.046	-.856	-.952	-1.251	-1.322
23	-1.295	-.336	-.255	-.221	-.065	-.392	-.784
24	-.804	-.212	-.167	-.047	-.054	-.140	-.359
25	.994	1.020	.445	-1.102	.024	.473	.433
26	.410	.565	.802	.472	*000.000	1.060	.865
27	-.048	.019	.347	.831	1.013	.817	.597
28	-.045	.049	.353	.764	.669	.495	.303
29	.243	.386	.519	.728	.655	.535	.439
30	.641	1.166	.718	.977	1.035	.986	.091
31	.925	1.117	.647	1.009	1.064	1.043	.650
32	.567	.761	.672	.821	.868	.769	.761
33	.288	.496	.506	.593	.627	.493	.026

$\alpha = 20°$

TUBE NO	WING STATIONS						
	1	2	3	4	5	6	7
1	.735	.577	-.418	-4.450	-3.694	-2.138	-2.074
2	-.142	-.502	-1.175	-5.624	-4.564	-3.549	-3.020
3	-.282	-.679	-1.172	-5.410	-5.058	-4.020	-3.360
4	-.920	-1.178	-1.433	-4.790	-4.603	-4.040	-3.599
5	-1.022	-1.471	-1.491	-3.561	-3.577	-3.222	-2.869
6	*000.000	*000.000	*000.000	*000.000	*000.000	*000.000	*000.000
7	*000.000	*000.000	*000.000	*000.000	*000.000	*000.000	*000.000
8	*000.000	*000.000	*000.000	*000.000	*000.000	*000.000	*000.000
9	*000.000	*000.000	*000.000	*000.000	*000.000	*000.000	*000.000
10	-1.009	-1.656	-1.542	-2.491	-2.368	-2.055	-1.733
11	-1.003	-1.511	*000.000	-1.628	-1.910	-1.611	-1.408
12	-1.191	-1.046	-.946	-.740	-1.189	-.981	-.775
13	-.874	-1.024	-.812	-.759	-.927	-.785	-.590
14	-1.142	-1.046	-.848	-.782	-.896	-.788	-.674
15	-.174	-.153	.393	.448	.385	.385	-.103
16	-.350	-.141	.075	.122	-.003	.022	-.164
17	-1.119	-1.164	-.626	-.648	-.917	-.665	-.605
18	-1.923	-1.884	-1.413	-1.249	-1.532	-1.483	-1.173
19	-2.728	-2.459	-1.978	-1.508	-1.616	-1.616	-1.119
20	-2.566	-2.634	-1.947	-1.364	-1.576	-1.648	-1.203
21	-3.055	-2.163	-1.699	-1.181	-1.556	-1.544	-1.353
22	-2.892	-1.728	-1.320	-.895	-1.075	-1.175	-1.214
23	-1.517	-.413	-.240	-.260	-.211	-.420	-.807
24	-1.052	-.294	-.116	-.032	.033	-.061	-.328
25	1.074	1.130	.447	-2.340	-.985	-.109	-.119
26	.671	.941	.533	.353	*000.000	1.011	.747
27	.049	.340	.576	.884	1.007	.940	.605
28	-.016	.340	.448	.798	.754	.612	.319
29	.065	.427	.586	.648	.583	.583	.384
30	.707	1.074	.900	.921	.916	.951	-.013
31	.666	1.158	1.038	1.017	1.032	1.047	.470
32	.579	.846	.855	.925	.895	.896	.790
33	.309	.544	.601	.649	.624	.566	.065

$\alpha = 25°$

TUBE NO	WING STATIONS						
	1	2	3	4	5	6	7
1	.512	.201	-1.074	-6.527	-5.123	-3.437	-2.835
2	-.445	-.933	-1.675	-6.840	-5.615	-4.288	-3.449
3	-.609	-1.498	-2.047	-6.941	-6.047	-4.357	-3.265
4	-1.244	-1.973	-2.202	-6.323	-5.754	-4.574	-3.713
5	-1.343	-1.951	-2.041	-4.444	-4.066	-3.256	-2.433
6	*000.000	*000.000	*000.000	*000.000	*000.000	*000.000	*000.000
7	*000.000	*000.000	*000.000	*000.000	*000.000	*000.000	*000.000
8	*000.000	*000.000	*000.000	*000.000	*000.000	*000.000	*000.000
9	*000.000	*000.000	*000.000	*000.000	*000.000	*000.000	*000.000
10	-1.195	-1.944	-1.763	-2.631	-2.383	-1.837	-1.196
11	-1.993	-1.516	*000.000	-1.573	-1.760	-1.295	-.816
12	-1.605	-1.710	-1.068	-.663	-1.125	-.751	-.668
13	-1.178	-1.149	-.982	-.817	-.933	-.781	-.725
14	-1.347	-1.161	-.911	-.749	-.818	-.684	-.491
15	-.523	-.123	.345	.512	.439	.409	-.050
16	-.553	-.184	.092	.194	.052	-.005	-.116
17	-1.447	-1.296	-.607	-.655	-.935	-.542	-.426
18	-2.151	-1.957	-1.508	-1.176	-1.317	-1.074	-.763
19	-3.176	-2.579	-2.191	-1.195	-1.324	-.940	-.655
20	-3.416	-2.667	-2.233	-1.445	-1.675	-1.556	-.958
21	-3.769	-2.557	-2.074	-1.074	-1.249	-.599	-.573
22	-3.425	-1.971	-1.448	-.901	-.937	-1.028	-.880
23	-1.477	-.371	-.291	-.210	-.203	-.347	-.565
24	-1.099	-.310	-.155	.009	-.097	-.386	-.409
25	1.171	1.222	.219	-3.304	-1.794	-.621	-.719
26	.442	1.212	.963	.244	*000.000	1.037	.431
27	.254	.623	.614	.971	1.040	1.000	.472
28	.065	.343	.559	1.014	.841	.642	.413
29	.633	.506	.575	.723	.602	.562	.433
30	.639	1.275	1.176	1.010	.943	.998	-.066
31	.782	1.226	1.135	1.035	1.046	1.101	.470
32	.537	.919	.942	.955	.883	.839	.740
33	.315	.616	.771	.755	.641	.507	.025

36

L-66-9862
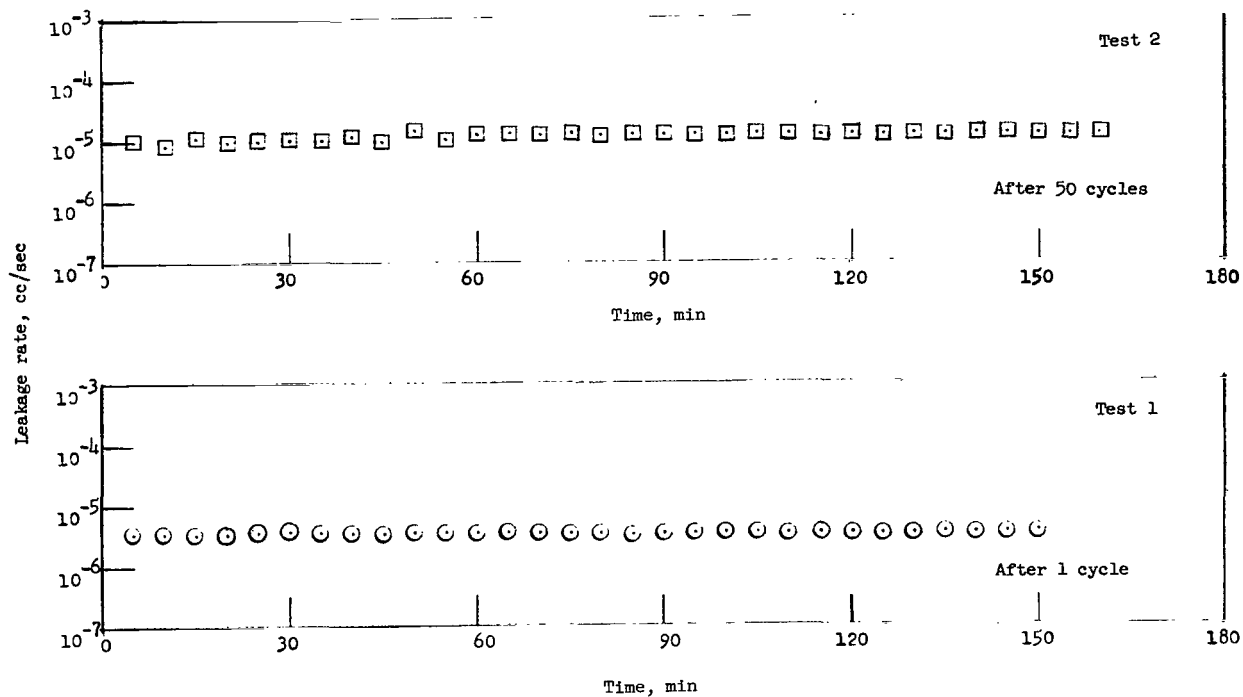
Figure 22.- Arrangement for cooling hatch C.

Figure 23.- Leakage rate as a function of time for hatch A with pressure loading toward the closed position.
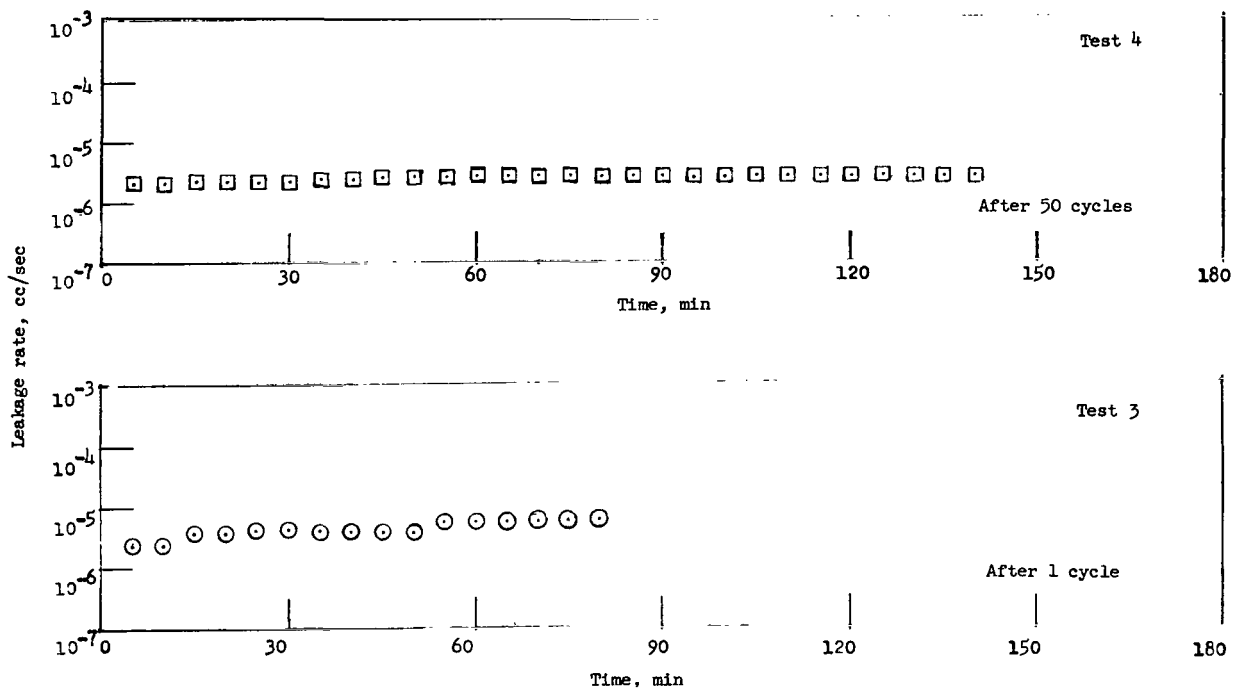

Figure 24.- Leakage rate as a function of time for hatch A with pressure loading toward the open position.
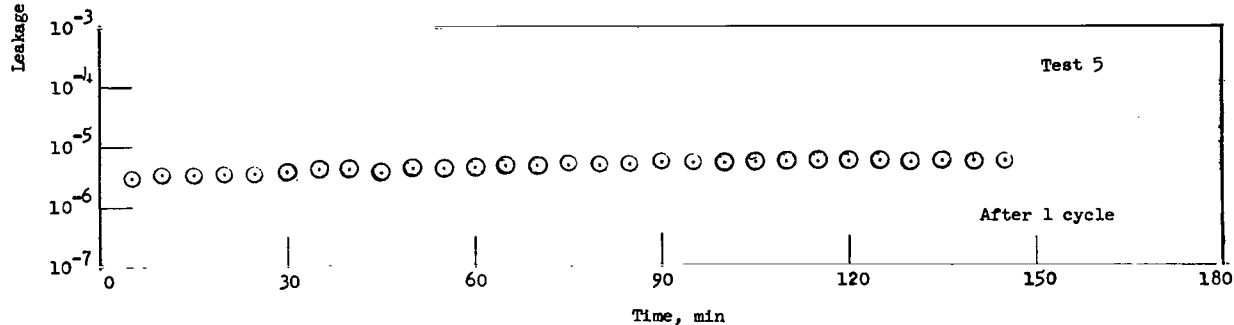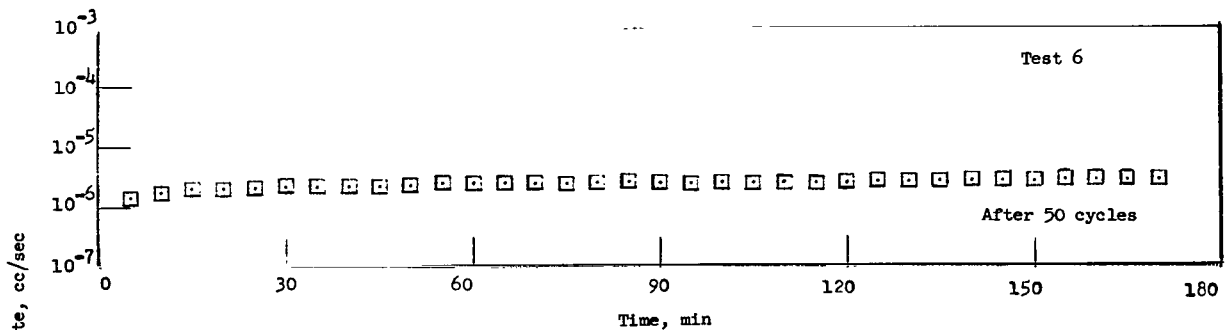
Figure 25.- Leakage rate as a function of time for hatch B with pressure loading toward the closed position.
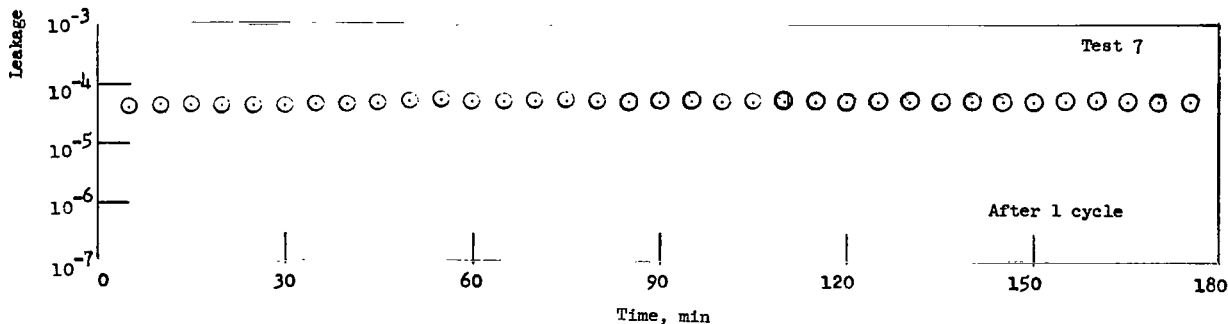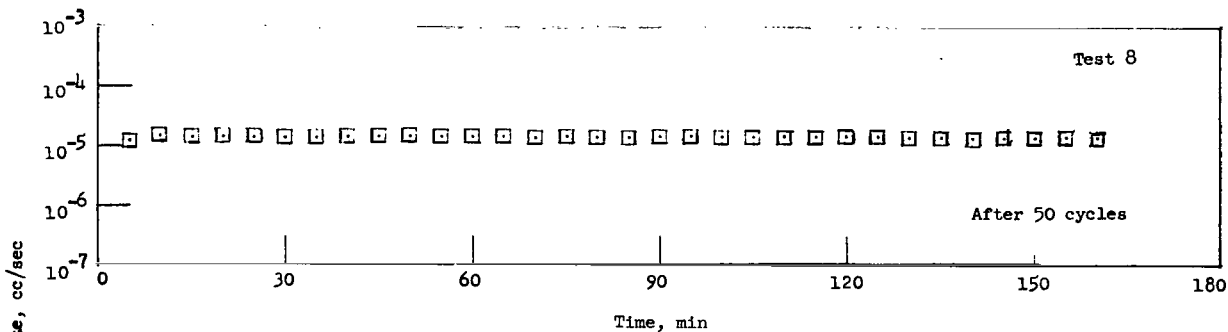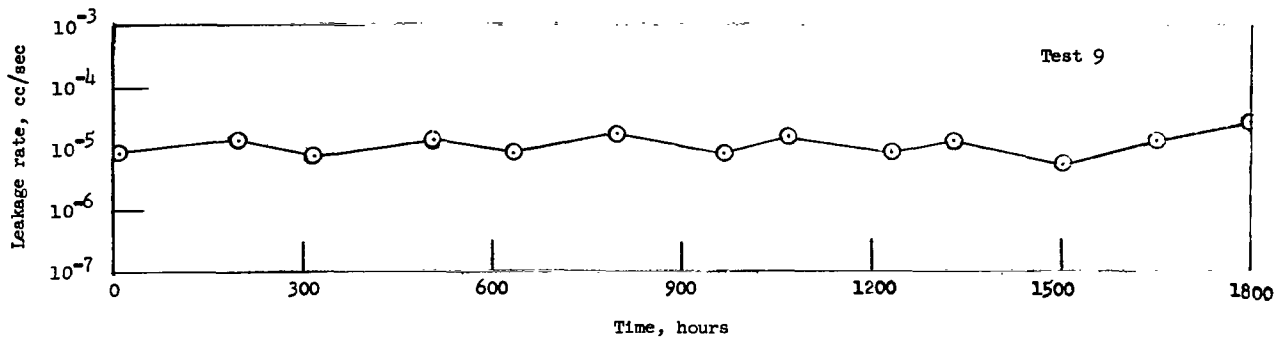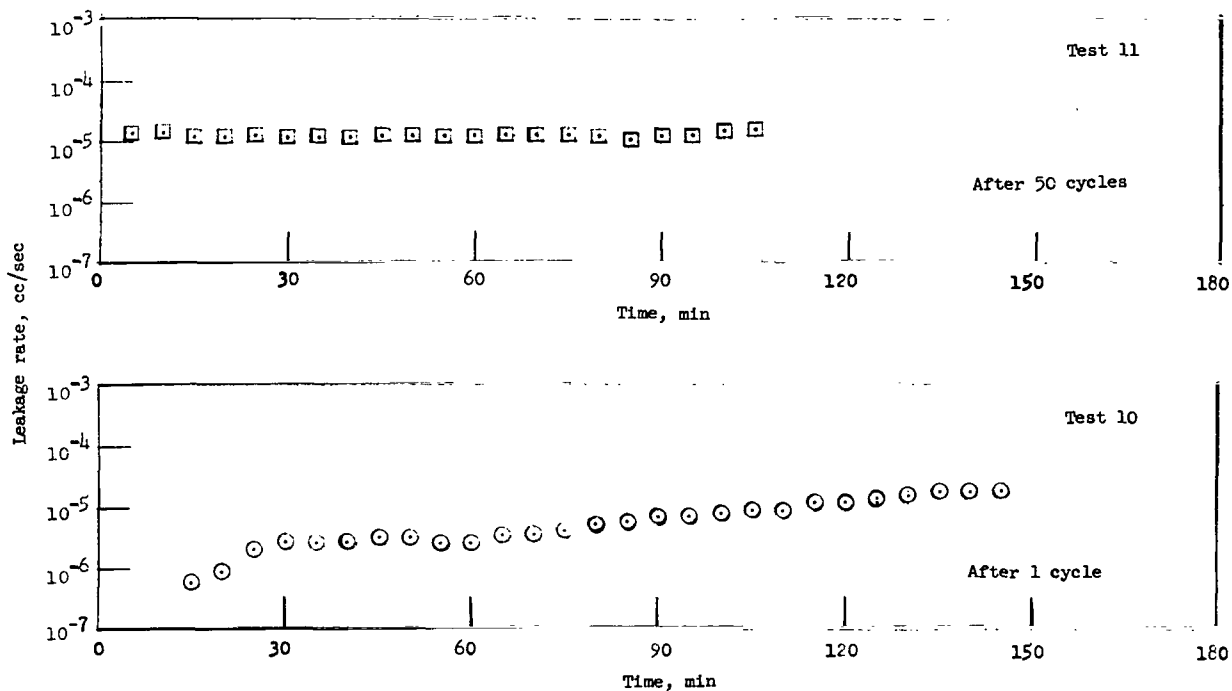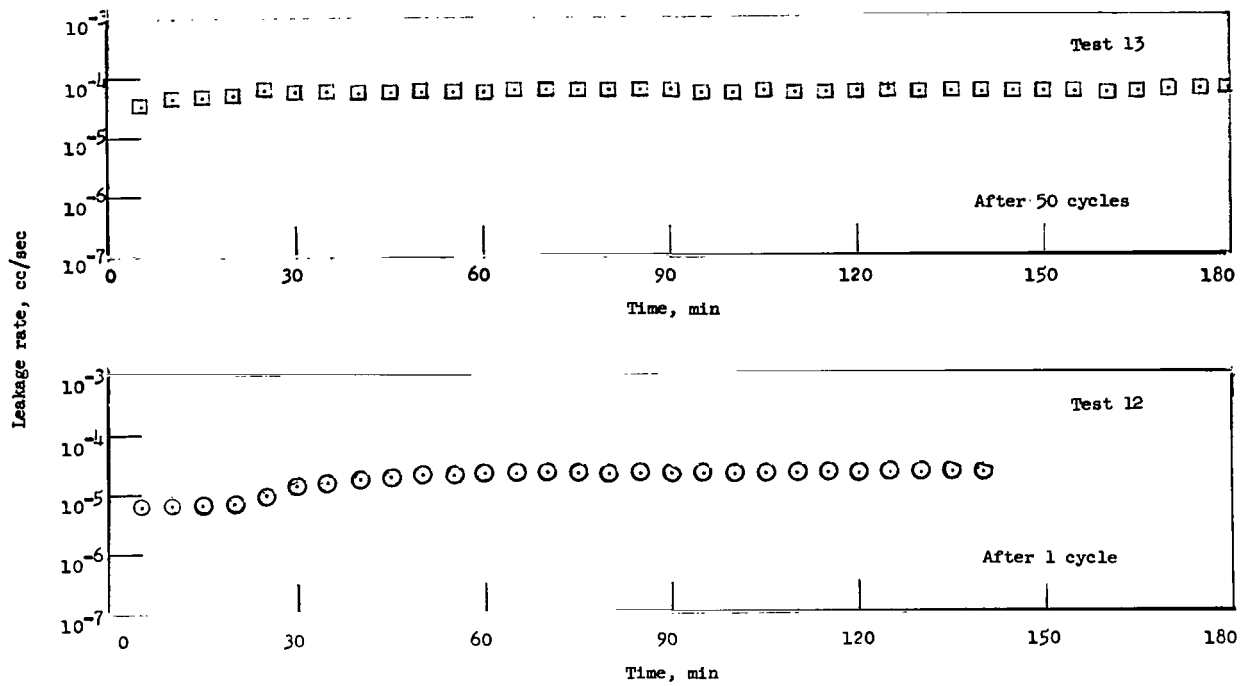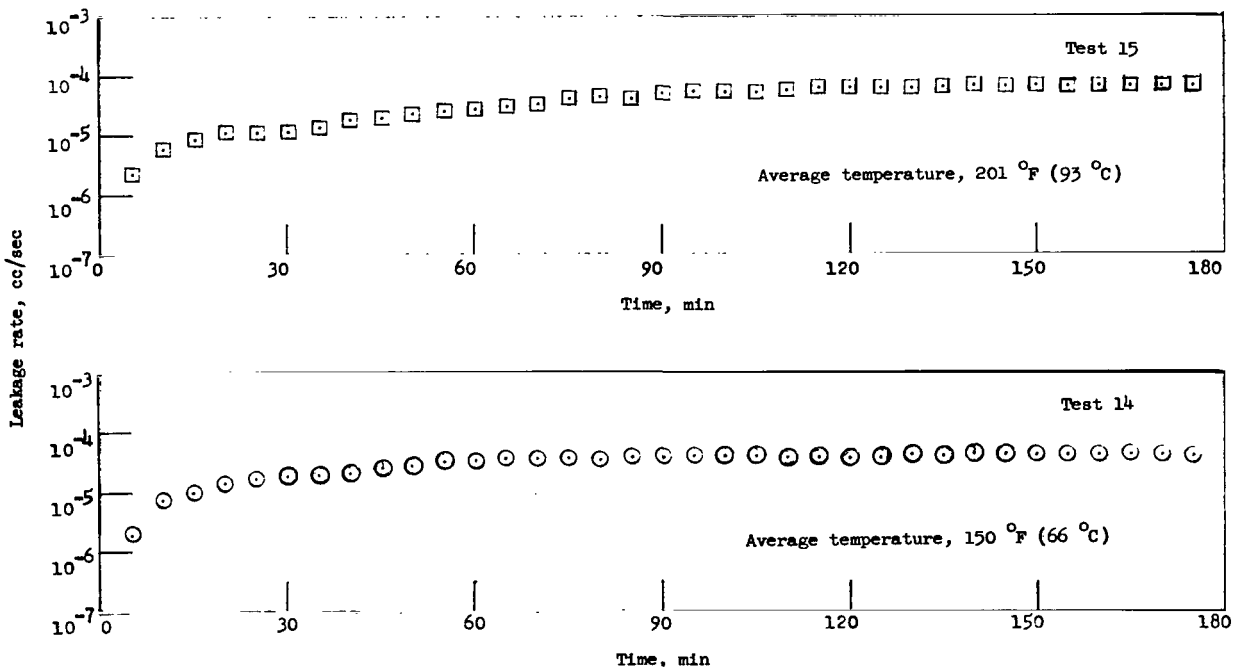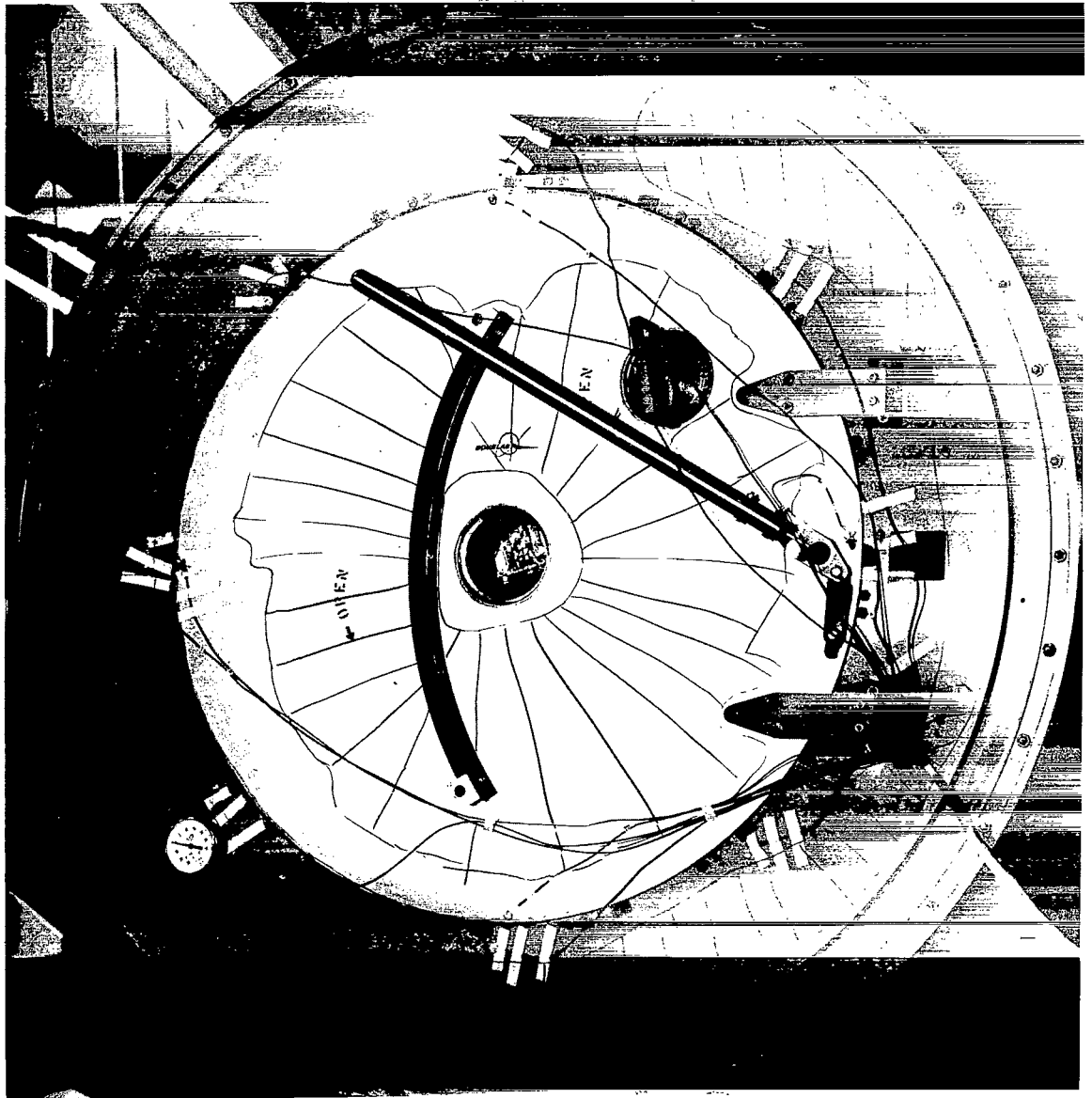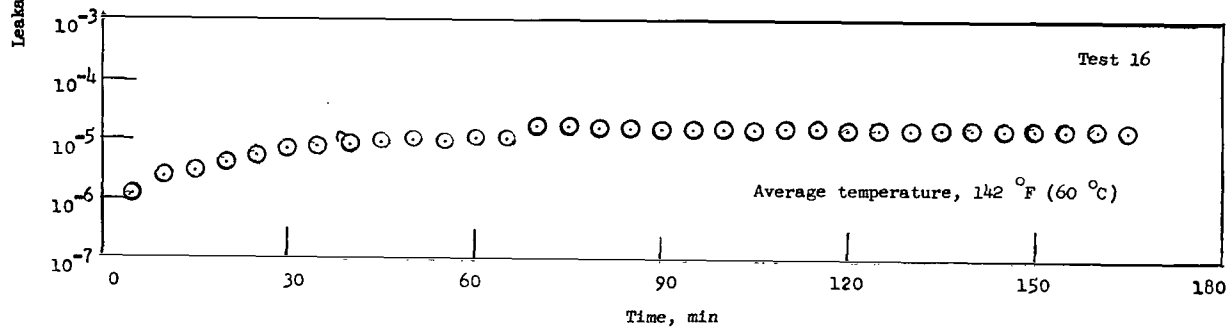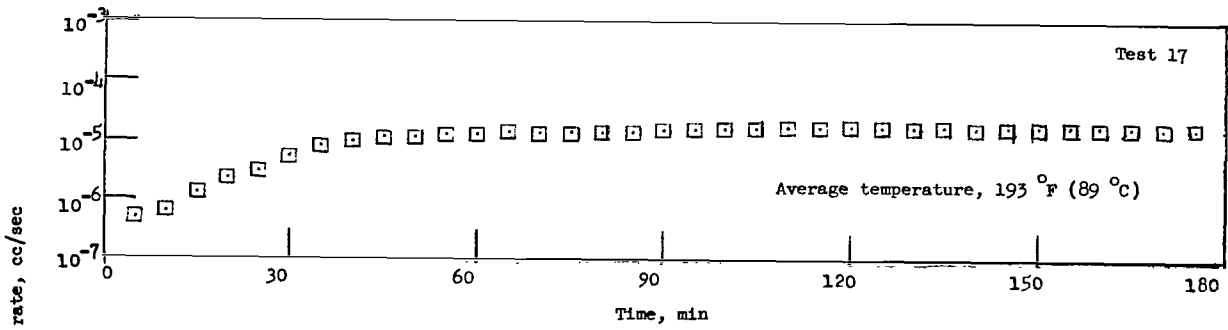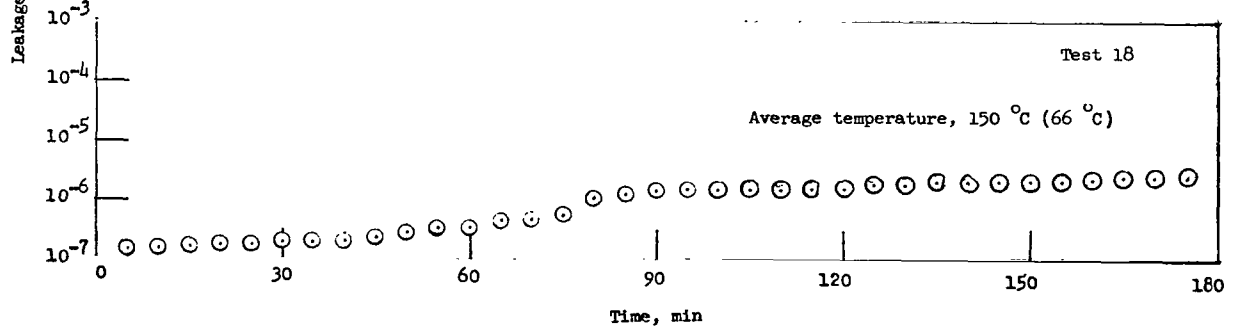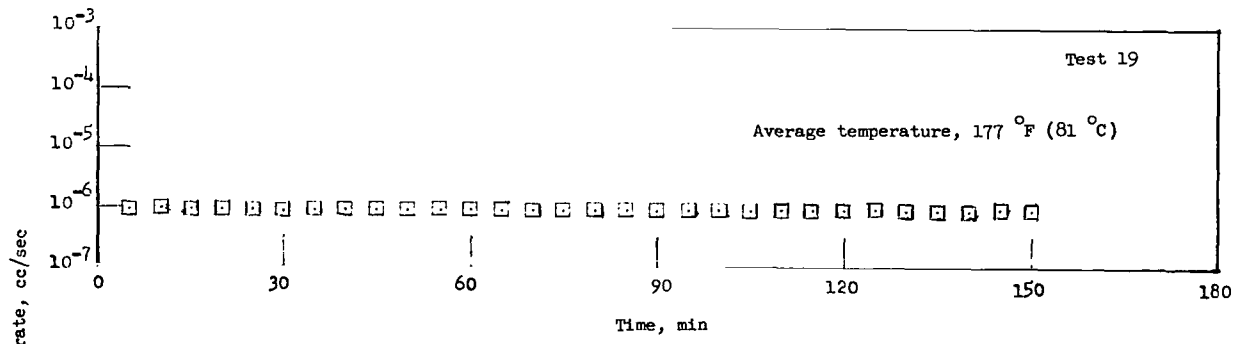

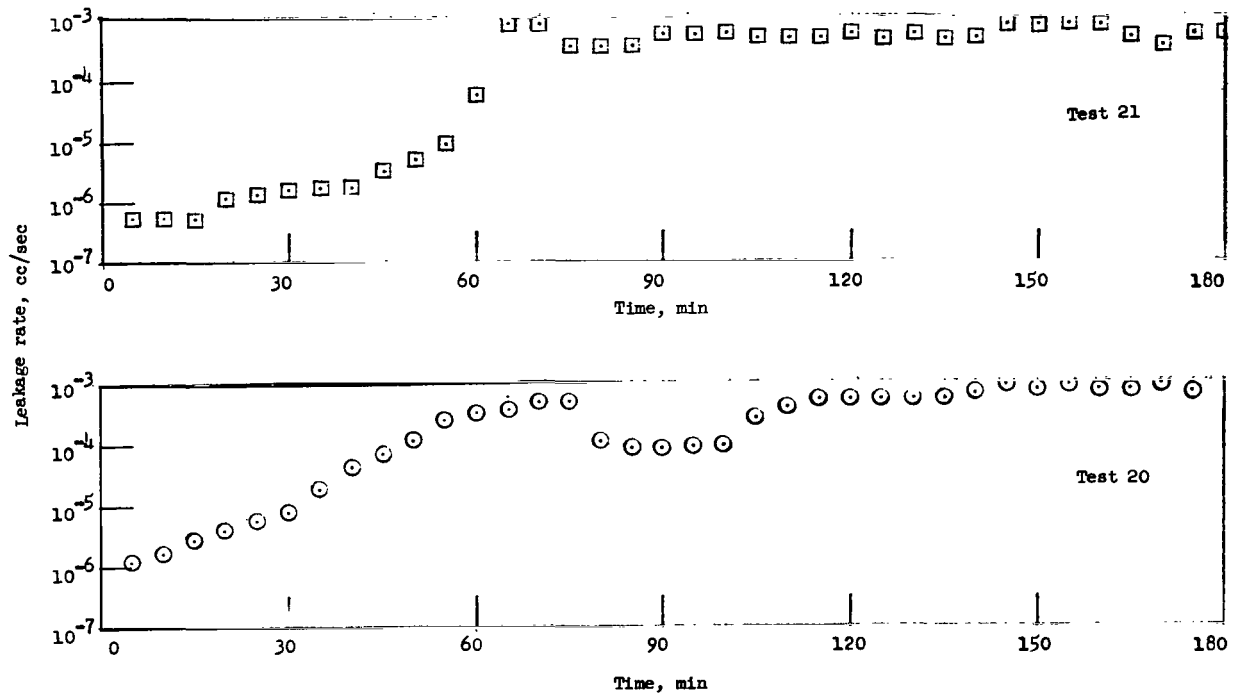Figure 26.- Leakage rate as a funtion of time for hatch B with pressure loading toward the open position.

39

Figure 27.- Leakage rate as a function of time for hatch B with pressure loading toward the closed position during the 75-day test.
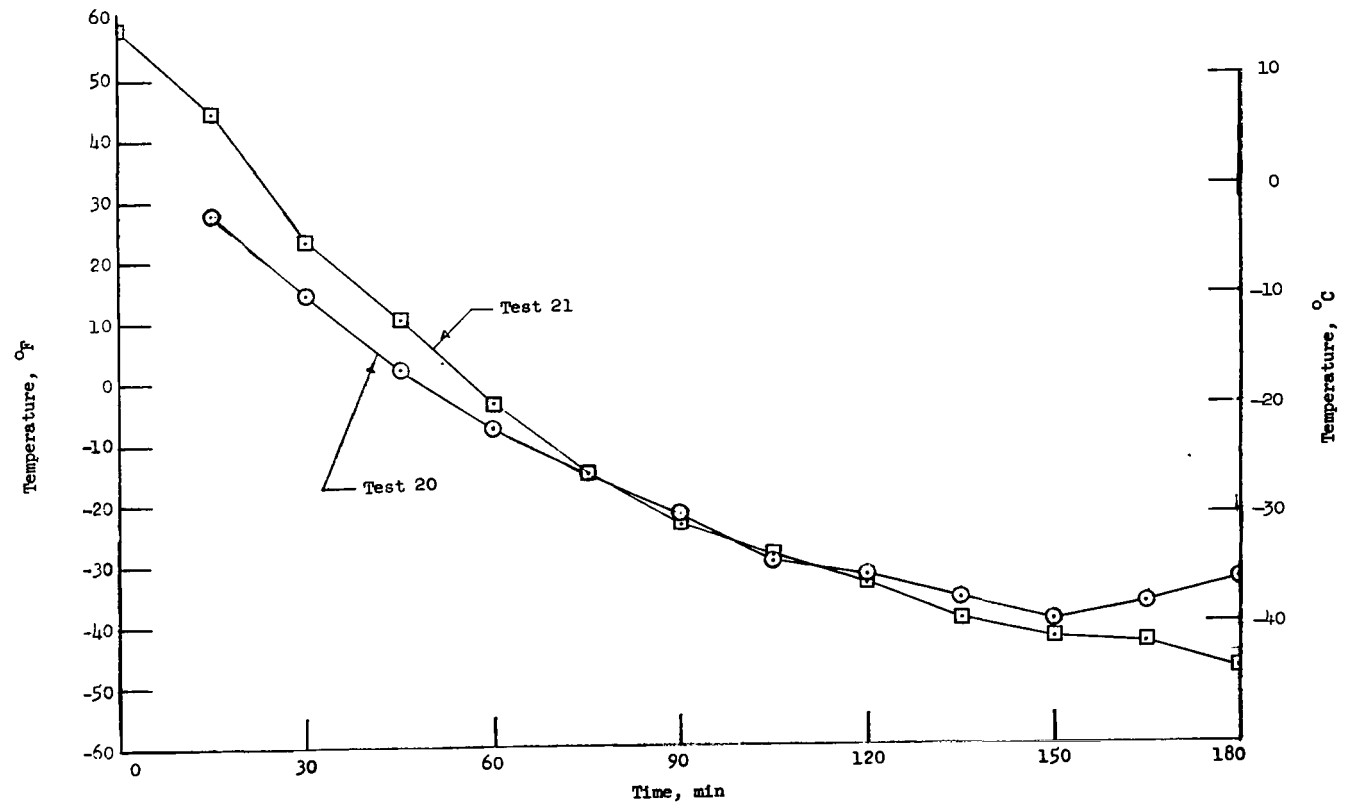

Figure 28.- Leakage rate as a function of time for hatch C with pressure loading toward the closed position.

Figure 29.- Leakage rate as a function of time for hatch C with pressure loading toward the open position.

Figure 30.- Leakage rate as a function of time for hatch A with pressure loading toward the closed position during the heating tests.

41

L-66-10106

Figure 31.- Failure areas of hatch A and frame.

Figure 32.- Leakage rate as a function of time for hatch B with pressure loading toward the closed position during the heating tests.
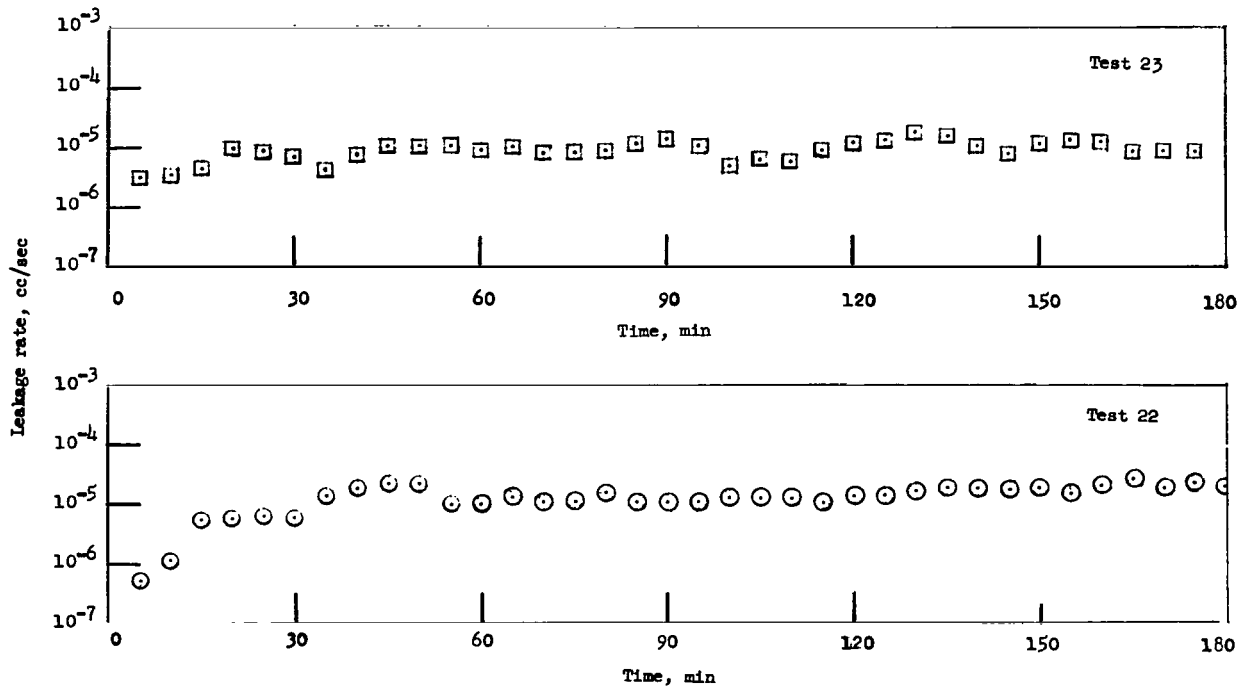
Figure 33.- Leakage rate as a function of time for hatch C with pressure loading toward the closed position during the heating tests.

Figure 34.- Leakage rate as a function of time for hatch B with pressure loading toward the closed position during the cooling tests.
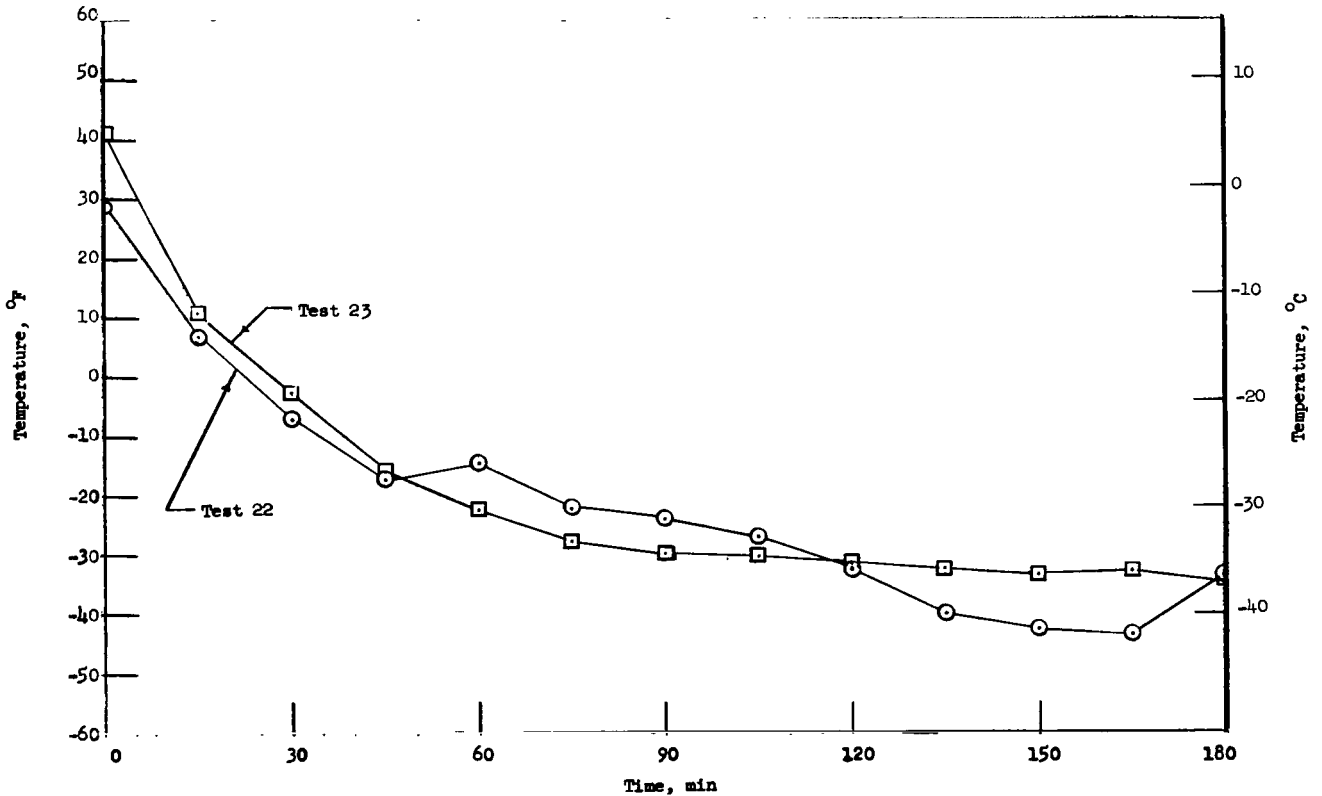

Figure 35.- Average temperature as a function of time for the structure surrounding the seal on hatch B during the cooling tests.

Figure 36.- Leakage rate as a function of time for hatch C with pressure loading toward the closed position during the cooling tests.

Figure 37.- Average temperature as a function of time for the structure surrounding the seal on hatch C during the cooling tests.

"The aeronautical and space activities of the United States shall be
conducted so as to contribute . . . to the expansion of human knowl-
edge of phenomena in the atmosphere and space. The Administration
shall provide for the widest practicable and appropriate dissemination
of information concerning its activities and the results thereof."

— NATIONAL AERONAUTICS AND SPACE ACT OF 1958

NASA SCIENTIFIC AND TECHNICAL PUBLICATIONS

TECHNICAL REPORTS: Scientific and
technical information considered important,
complete, and a lasting contribution to existing
knowledge.

TECHNICAL NOTES: Information less broad
in scope but nevertheless of importance as a
contribution to existing knowledge.

TECHNICAL MEMORANDUMS:
Information receiving limited distribution
because of preliminary data, security classifica-
tion, or other reasons.

CONTRACTOR REPORTS: Scientific and
technical information generated under a NASA
contract or grant and considered an important
contribution to existing knowledge.

TECHNICAL TRANSLATIONS: Information
published in a foreign language considered
to merit NASA distribution in English.

SPECIAL PUBLICATIONS: Information
derived from or of value to NASA activities.
Publications include conference proceedings,
monographs, data compilations, handbooks,
sourcebooks, and special bibliographies.

TECHNOLOGY UTILIZATION
PUBLICATIONS: Information on technology
used by NASA that may be of particular
interest in commercial and other non-aerospace
applications. Publications include Tech Briefs,
Technology Utilization Reports and Notes,
and Technology Surveys.

Details on the availability of these publications may be obtained from:

SCIENTIFIC AND TECHNICAL INFORMATION DIVISION

NATIONAL AERONAUTICS AND SPACE ADMINISTRATION
Washington, D.C. 20546